Fermi-Einstein condensation in dense QCD-like theories

Kurt Langfeld[a], Andreas Wipf[b]

[a] School of Computing & Mathematics, University of Plymouth
Plymouth, PL4 8AA, UK

[b]Theoretisch-Physikalisches Institut, Friedrich-Schiller-Universität Jena
07743 Jena, Germany

Abstract

While pure Yang-Mills theory feature the centre symmetry, this symmetry is explicitly broken by the presence of dynamical matter. We study the impact of the centre symmetry in such QCD-like theories. In the analytically solvable Schwinger model, centre transitions take place even under extreme conditions, temperature and/or density, and we show that they are key to the solution of the Silver-Blaze problem. We then develop an an effective SU(3) quark model which confines quarks by virtue of centre sector transitions. The phase diagram by confinement is obtained as a function of the temperature and the chemical potential. We show that at low temperatures and intermediate values for the chemical potential the centre dressed quarks undergo condensation due to Bose like statistics. This is the *Fermi Einstein condensation.* To corroborate the existence of centre sector transitions in gauge theories with matter, we study (at vanishing chemical potential) the interface tension in the three-dimensional $\mathbb{Z}_2$ gauge theory with Ising matter, the distribution of the Polyakov line in the four-dimensional SU(2)-Higgs model and devise a new type of order parameter which is designed to detect centre sector transitions. Our analytical and numerical findings lead us to conjecture a new state of cold, but dense matter in the hadronic phase for which Fermi Einstein condensation is realised.

Contents

1 Introduction:

A great deal of efforts, theoretical and experimental, are devoted to explore the properties of hadronic matter under extreme conditions, temperature and/or baryonic densities. The general belief is that matter is organised in a quark-gluon plasma phase in this regime. At least for small densities, this belief is corroborated by lattice gauge calculations [1–3] and collision experiments such as undertaken at RHIC [4, 5].

Central to understand matter under extreme conditions is the understanding of colour confinement since its realisation is, almost by definition, the most prominent difference between the so-called hadronic and the quark-gluon plasma phase. Early on in the eighties, it was pointed out that the centre of the gauge group plays a major role for confinement: Realisation of the centre symmetry of the gauge sector goes in line with confinement while its spontaneous breakdown (e.g. at high temperatures) signals colour liberation [6, 7]. Roughly at the same time, it was proposed that certain degrees of freedom of Yang-Mills theories, such as monopoles or vortices, are responsible for the (dis-)order of the centre symmetry (see [8] for a review). It took until the late nineties to isolate these degrees of freedom in lattice gauge theories in a physical, i.e., regulator independent way [9, 10]. It was pointed out in [11] that the mere existence of centre vortices as physical degrees of freedom demand a fine tuning between vortex entropy and energy. Quite recently [12], smooth stream-line configurations which bear confinement have been found using lattice gauge simulations: it was pointed out that if centre vortices are images of these stream-line configurations in a certain gauge, it would naturally account for the intrinsic fine-tuning. Most importantly, the centre vortex picture offers an understanding of confinement on the basis of weakly interacting degrees of freedom, which explain high temperature deconfinement and the centre disorder of spatial correlations at the same time [13–15].

Although a quite detailed picture of confinement and deconfinement at finite temperatures has emerged over the last decade, very little is known about cold but dense matter from first principles. Because of the notorious "sign"-problem, Monte-Carlo simulations of Yang-Mills theories with dense quark matter are only feasible for SU(2) colour [16] for which the sign problem is absent[1] or for rather small densities (see [18] for a recent review). First insights into the properties of matter which feature in cold but dense QCD might be gained from exact solutions of models which mimic certain aspects of QCD. As an example, we mention the Gross-Neveu model which features the baryon crystal as an hitherto unknown state of matter [19–21].

Among the very few gauge theories which admit an exact solution even for the case of dense quark matter is 2d Quantumelectrodynamics, the so-called Schwinger model [22]. The model with massless fermions was exactly solved in Hamiltonian formalism on the line in [23–25] and on S^1 in [26, 27]: chiral symmetry is spontaneously broken and only states with a vanishing net baryon number appear in the spectrum. The model on the torus has

---

[1]G_2 Yang-Mills theory with dynamical fermions has no sign-problem as well and simulations at finite temperature and density are under way [17].

been studied in [28] and in particular the temperature dependence of the chiral condensate, Wilson loop correlators and Polyakov line correlators have been determined [29–31]. In [32, 33], non-vanishing values of the fermion chemical potential have been firstly considered. It was found, most importantly, that the full non-perturbative partition function is independent of the chemical potential. Since then, many more quantities have been obtained in the massless Schwinger model ranging from the temperature dependence of the correlators of hadronic currents, spectral functions to the screening mass [34]. This makes the Schwinger mode the ideal testbed to test new ideas, and we will make extensive use of this below.

Besides of exactly solvable models, understanding *mechanisms*, which have been revealed in model studies or by non-perturbative approximations, is an invaluable tool since they might extend their applicability to the theory of interest, in particular, cold and dense QCD matter. Recent examples are the proposal of the *quarkyonic* phase the existence of which has been motivated by the large N_c considerations (N_c being the number of colours) [35, 36]. Another recent example is the chiral magnetic effect which describes an induced electromagnetic current alongside an external magnetic field made possible by topological charge transitions in the quark gluon plasma phase [37, 38].

Of particular importance for this publication is the recent observation that quarks effectively comply to *periodic boundaries conditions* if exposed to a particular non-trivial centre sector in $SU(N_c)$ Yang-Mills theory for N_c even. In the dense hadronic (confining) phase, this opens the possibility that centre dressed quarks undergo condensation reminiscent of Bose-Einstein condensation [39]. In analogy, this has been called *Fermi Einstein condensation (FEC)* [40]. We also point out that the sensitivity of the quark spectrum to the boundary conditions of the quarks has been studied in [41].

In this paper, we will further study the phenomenological impact of the FEC effect. We will use the Schwinger model which will allow to study FEC on almost purely analytical grounds. Since in previous studies we considered an even number of colours, we here extend the considerations to the more relevant case of an $SU(N_c = 3)$ gauge group using a quark model. We are going to show that transitions between the centre sectors are sufficient to confine quarks in this model. The quark model itself determines the so-called centre sector weights which serve as an order parameter for confinement. Using these weights, we will be able to calculate the phase diagram of the model as a function of the chemical potential and the temperature. For $N_c = 3$, we find that FEC does occur under cold and dense conditions at the presence of pressure. Essential for FEC is that the gluonic states manoeuvre through the centre sectors. Since non-trivial centre-sectors are suppressed by the presence of dynamical matter, we accumulate evidence in the remainder of the paper that centre sector transitions do occur in the so-called hadronic phase. To this aim, we will study the $\mathbb{Z}_2$ gauge theory with Ising matter and the SU(2) Higgs theory. We develop a novel order parameter which is sensitive to centre sector transitions and provide numerical evidence that these transitions take place until centre symmetry is spontaneously broken at high temperatures.

4

The paper is organised as follows: In section 2, we extend the considerations of [42–44] and show that the Yang-Mills "empty" vacuum possess gauge in-equivalent flat directions which collapse to the so-called centre-sectors once quantum fluctuations are included. Section 3 addresses FEC in the context of the Schwinger model. In section 4, we develop the $SU(3)$ quark model with confinement by virtue of the interaction of the quarks with the centre sector background fields. Confinement is established by studying the model's thermal excitations, and the phase diagram from confinement is obtained. In section 5, we start to investigate centre-sector transition by means of numerical simulations. For this purpose, we study the $\mathbb{Z}_2$ gauge theory with Ising matter, which has not yet been studied before to our knowledge. In section 6, we extend the simulations and consider the SU(2) Higgs theory. The order parameter for centre sector transitions is developed and our numerical findings for this order parameter are presented. Conclusions are left to the final section.

2 Yang-Mills moduli space and centre sectors

2.1 The empty vacuum on a torus

A configuration with minimal Euclidean action, often called *empty* vacuum, is often the starting point of perturbation theory. In Abelian theories, it is naturally defined as a state for which the field strength at any point of space-time vanishes. In non-Abelian theories, such as $SU(N_c)$ Yang-Mills theories, a more stringent definition is in order: there, the empty vacuum is a state for which the holonomy calculated along any contractible loop $\mathcal{C}$ yields the unit element of the gauge group:

$$ \mathrm{P} \, \exp\left\{ \mathrm{i} \int_{\mathcal{C}} A_\mu(x)\, dx^\mu \right\} \; = \; \mathbb{1} \qquad \text{(empty vacuum condition)}, \tag{1} $$

where $A_\mu(x)$ is the gauge potential and P denotes path-ordering. Throughout this paper, we will consider a 4-torus as space-time manifold. The gauge potentials $A_\mu(x)$ and gauge transformations $\Omega(x)$ satisfy periodic boundary conditions[2], matter fields such as a scalar Higgs field $\phi(x)$ or quarks $q(x)$ are subjected to periodic and anti-periodic boundary conditions, respectively. We will adopt a lattice regularisation with the lattice spacing a acting as an UV regulator. Thereby, the gauge degrees of freedom are represented by the links $U_\mu(x) \in SU(N_c)$. Gauge transformations act as usual:

$$ U_\mu^\Omega(x) \; = \; \Omega(x)\, U_\mu(x)\, \Omega^\dagger(x+\mu) \, . \tag{2} $$

In lattice discretisation, the vacuum condition (1) becomes

$$ \prod_{\ell \in \mathcal{C}} U_\ell \; = \; \mathbb{1} \, , \qquad \ell = (x, \mu) \, , \tag{3} $$

where $\mathcal{C}$ is a closed and *contractible* path on the lattice. The smallest contractible loops on the lattice are the loops surrounding the elementary plaquettes of the lattice. For the

---

[2]In the continuum theory this implies a vanishing instanton number.
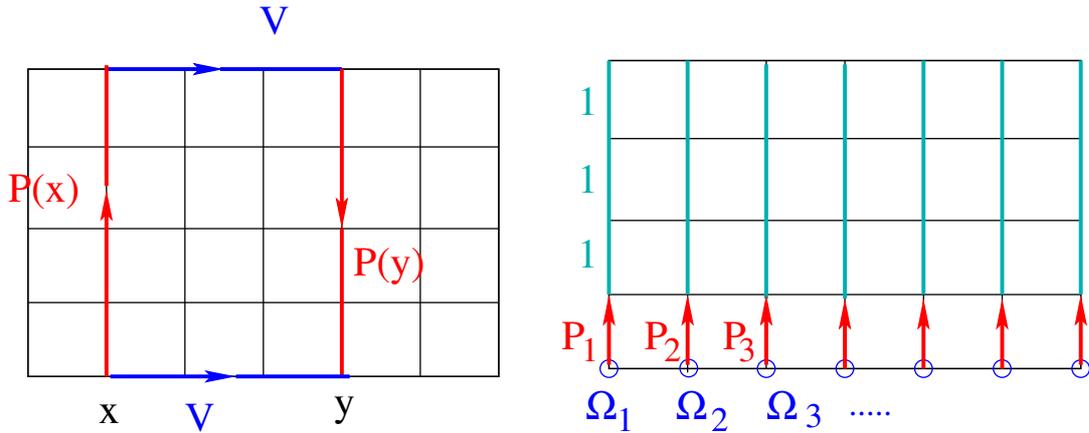
Figure 1: Absence of Polyakov line correlations in the "empty" vacuum (left). Step 1 of the complete gauge fixing (right).

later choice, the vacuum condition (3) implies that the non-Abelian field strength vanishes for the empty vacuum.

Already in the late nineties, it has been discovered that there are smoothly connected configurations which are gauge *in-equivalent* and which all satisfy the vacuum condition (1) (or (3)) [42–44]. The set of these configurations defines the Yang-Mills moduli space. While Keurentjes et al. discuss 3-dimensional Yang-Mills theory, the arguments were extended to 4-dimension in [44]. To make the paper self-contained, we will give a full account of the Yang-Mills moduli space using lattice regularisation.

Of particular importance for the study of confinement in Yang-Mills theories on the torus is the Polyakov line:

$$\mathcal{P}(\boldsymbol{x}) \; = \; \prod_t U_0(t, \boldsymbol{x}) \; . \tag{4}$$

Let us firstly study their correlations in the empty vacuum. For this purpose, we consider the maximal (contractible) loop in figure 1, left panel (note that the product V of spatial links is the same at the lower and upper time-slices due to periodic boundary conditions). The vacuum condition implies

$$\mathcal{P}(\boldsymbol{x})V\mathcal{P}^{\dagger}(\boldsymbol{y})V^{\dagger} \; = \; \mathbb{1} \qquad \Rightarrow \qquad \operatorname{tr}\mathcal{P}(\boldsymbol{x}) \; = \; \operatorname{tr}\mathcal{P}(\boldsymbol{y}). \tag{5}$$

Hence, the trace of the Polyakov line is necessarily constant for any choice of an "empty" vacuum. Given that the static quark anti-quark potential $V(r)$ can be extracted from the Polyakov line correlator:

$$\langle P(\boldsymbol{x})\,P(\boldsymbol{y})\rangle \propto \exp\left\{-V(r)/T\right\}, \qquad P(\boldsymbol{x}) = \frac{1}{N_c}\operatorname{tr}\mathcal{P}(\boldsymbol{x}), \tag{6}$$

where $r = |\boldsymbol{x} - \boldsymbol{y}|$ and T is the temperature, the finding (6) implies that a single "empty" state cannot sustain quark confinement.

6
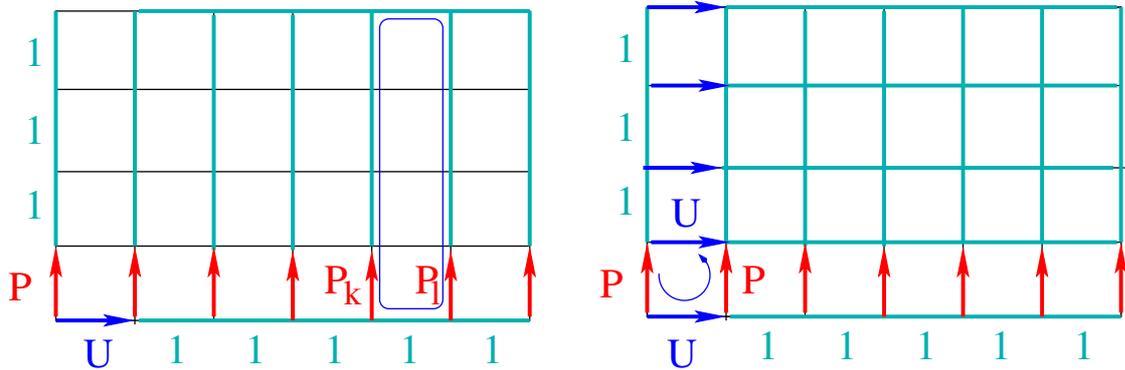
Figure 2: Gauge fixing step 2 (right) and (almost) completely gauge fixed configuration (left).

Genuinely different vacua states are obtained by identifying all states which are related by gauge transformations. In order to calculate those, a complete unique gauge fixing is in order. In a first step, we adopt a Polyakov type of gauge fixing: all time like links $U_0(t, \boldsymbol{x})$ for $t > 1$ are gauged to the unit element (see figure 1, left panel). The only non-trivial time-like links are those at $t = 1$, which thus equal the Polyakov line. The gauge transformation Ω_1, Ω_2, etc, are not used for this first gauge fixing step. These gauge transformations are now employed to gauge almost all spatial links at time-slice $t = 1$ to the unit element (see figure 2, right panel). The empty vacuum condition then implies that all spatial links without arrows in figure 2 are transformed to the unit element. The spatial links U which are far most to the left then equal the spatial Polyakov line in this direction. We then again use the vacuum condition for the contractible loop in figure 2, left panel and conclude that

$$\mathcal{P}(\boldsymbol{x}_k) \, \mathbb{1} \, \mathcal{P}^\dagger(\boldsymbol{x}_\ell) \, \mathbb{1} = \mathbb{1} \qquad \Rightarrow \qquad \mathcal{P}(\boldsymbol{x}_k) = \mathcal{P}(\boldsymbol{x}_\ell) = \mathcal{P} \,.$$

In this gauge and for an empty vacuum state, not only the *trace* of the Polyakov is constant but also the full Polyakov line including off-diagonal parts. After the above gauge fixing, only gauge transformation Ω_1 remains unfixed and acts as a residual *global* colour symmetry. In a final step, we consider the plaquette in the bottom left corner of the lattice in figure 2, right panel. Generically, the eigenvalues of the spatial and time-like Polyakov lines are different. In order to satisfy the vacuum condition for this case, the matrices $\mathcal{P}$ and U are drawn from the Cartan subgroup of $SU(N_c)$ implying:

$$\mathcal{P} U \mathcal{P}^\dagger U^\dagger = \mathbb{1} \qquad \Rightarrow \qquad [\mathcal{P}, U] = 0 \,.$$

Let the spatial Polyakov line U now be an element of the Cartan subgroup with all eigenvalues different. The Polyakov line $\mathcal{P}$ must then be an element of the Cartan subgroup in order to describe an empty vacuum:

$$\mathcal{P} \;\in\; [U(1)]^{N_c-1} \,.$$

7

For two choices of $\mathcal{P}$ with at least one eigenvalue being different, we obtain two *gauge in-equivalent* empty vacua states. Note that the Polyakov line homogeneously transforms under gauge transformations,

$$\mathcal{P}^\Omega(\boldsymbol{x}) \;=\; \Omega(\boldsymbol{x})\mathcal{P}(\boldsymbol{x})\Omega^\dagger(\boldsymbol{x}) \,,$$

implying that its eigenvalues are gauge invariant. Each $U(1)$ is spanned by a compact angle variable α_n, $n = 1 \ldots N_c - 1$, which span the space of global minima of the classical Yang-Mills action - the moduli space. For each direction, the corresponding Polyakov line can be chosen from the $[U(1)]^{N_c-1}$ subgroup. Hence, the moduli space is at least spanned by the

$$[U(1)]^{d(N_c-1)}$$

group manifold. Note that if, for a particular direction, the eigenvalues of the Polyakov line are f fold degenerate, the Polyakov lines of the other direction can be chosen from a $SU(f)$ subgroup and still satisfy the empty vacuum condition. Hence, the moduli space is slightly larger than the space spanned by the $U(1)$ groups only.

We finally make two comments:

(i) We point out that the *trace* of the Polyakov line being different is a *sufficient*, but not a *necessary* condition for two states being at different points in moduli space: assume that two Polyakov lines possess different eigenvalues but the same sum of all eigenvalues. They would belong to different points in moduli space, but their trace would be equal.

(ii) A perturbative treatment should involve a summation over all states with minimal (global) action. This implies an integration over the moduli space. Note that the standard perturbation theory merely chooses one state (i.e., the state of vanishing gauge potential or the state of all unit links in lattice formulation) of the moduli space. The integration over the moduli space would most likely remove the colour states from the theory thus inducing confinement. It would not, however, provide a confinement scale. Perturbation theory with an integration over the moduli space as well as the phenomenological implications of the moduli space integrations in effective quark theories will be explored elsewhere.

2.2 Yang-Mills quantum vacuum

The flat directions of the "empty" vacuum, discussed in detail in the previous subsection, are lifted if quantum fluctuations are considered. The symmetry of the quantum effective action collapses to the discrete centre symmetry. Introducing the centre elements of $SU(N_c)$ by

$$z_m \;=\; \exp\Big\{\mathrm{i}\,\frac{2\pi}{N_c}\,m\Big\}, \qquad m = 1 \ldots N_c, \tag{7}$$

the centre transformed lattice configuration $\{U^c\}$ is obtained by multiplying all time-like links at a given time slice t_0 by z_m:

$$U_0^c(t_0, \boldsymbol{x}) \;=\; z_m\, U_0(t_0, \boldsymbol{x}) \,, \qquad \text{for} \quad \forall \boldsymbol{x} \,, \tag{8}$$
$$U_\mu^c(t, \boldsymbol{x}) \;=\; U_\mu(t, \boldsymbol{x}) \,, \qquad \text{else} \,. \tag{9}$$

If the lattice action in pure Yang-Mills theory consists of a collection of contractible loops (such as the Wilson action which is constructed from the smallest of such loops - the plaquette), the action is invariant under the above centre transformation. On the other hand, the Polyakov line (4) transform homogeneously:

$$\mathcal{P}[U^c](\boldsymbol{x}) \;=\; z_m\,\mathcal{P}[U](\boldsymbol{x}) \;. \tag{10}$$

Any ergodic Monte-Carlo simulation on a finite lattice necessarily averages over the centre copies in a democratic way implying that

$$\langle P[U]\rangle \;=\; \langle P[U^c]\rangle \;=\; z_m\,\langle P[U]\rangle \qquad\Rightarrow\qquad \langle P[U]\rangle = 0\;,$$

which is also true in the high temperature phase of Yang-Mills theory. Showing that centre sector transitions imply confinement hence request more subtle arguments involving centre invariant expectation values.

To this aim, let us directly consider the static quark antiquark potential $V(r)$ as inferred from the Polyakov line correlation function (6). Instead of the Polyakov line expectation value, we consider its spatial average in relation to a reference $P(0)$ on the lattice. We observe

$$\left\langle P(0)\sum_{\boldsymbol{x}}P(\boldsymbol{x})\right\rangle \;\propto\; \sum_{\boldsymbol{x}}\mathrm{e}^{-V(r)/T} \;=\; \text{finite} \qquad\Rightarrow\qquad \lim_{r\to\infty}V(r)\to\infty\;,$$

and, hence, confinement. If on the other hand the potential approaches a finite value for $r\to\infty$, the correlator necessarily behaves as

$$\lim_{r\to\infty}\left\langle P(0)\,P(\boldsymbol{x})\right\rangle \;=\; \text{finite} \qquad\text{or}\qquad \left\langle P(0)\sum_{\boldsymbol{x}}P(\boldsymbol{x})\right\rangle \to\infty\;. \tag{11}$$

In view of (10), the latter equation could mean that centre sector disorder does not occur at length scales set by the lattice size. In the next subsection, we will show that the latter condition is in line with what is usually referred to as the spontaneous breakdown of centre symmetry. This breakdown occurs at high temperatures leaving us with the so-called quark-gluon plasma phase.

2.3 Spontaneous breaking of centre symmetry

One way to reveal the spontaneous breaking of centre symmetry using ergodic Monte-Carlo simulations is to add a centre symmetry breaking source term to the action and controlling the strength of this term by a parameter, let us say, h, which is reminiscent of a magnetic field in an Ising type setting. To be explicit, we will study SU(2) lattice gauge theory using a Euclidean space-time lattice represented by a $N_s^3\times N_t$ grid with lattice spacing a. Using
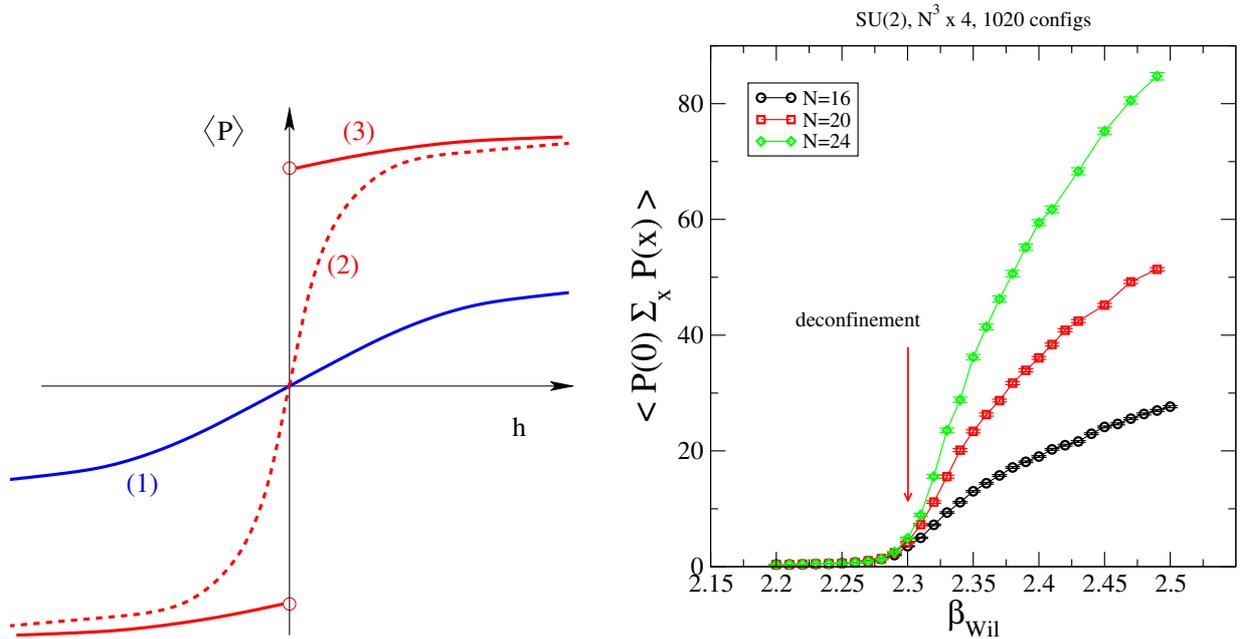
Figure 3: Sketch of the response of the Polyakov line expectation value to external centre symmetry breaking (left). The response function of the Polyakov line to an external field as function of β_{Wil} for several spatial volumes (right).

the Wilson action, the partition function is given

$$
\begin{aligned}
Z_{\text{YM}} &= \int \mathcal{D}U \ \exp\{S_{\text{Wil}} + S_{\text{break}}\} , &\text{(12)}\\
S_{\text{Wil}} &= \frac{\beta_{\text{Wil}}}{N_c} \sum_{x,\mu<\nu} \text{tr} \left\{ U_\mu(x) \, U_\nu(x+\mu) \, U_\mu^\dagger(x+\nu) \, U_\nu^\dagger(x) \right\} , \\
S_{\text{break}} &= h \sum_{\boldsymbol{x}} P(\boldsymbol{x}) ,
\end{aligned}
$$

where we have used the Polyakov line (4) to test the response of the theory to explicit centre symmetry breaking.

In the confinement phase, the Polyakov line expectation value $\langle P \rangle$ linearly responds to the presence of an external centre symmetry breaking. This is illustrated in figure 3, left panel, curve (1). Let us now consider the quark gluon plasma, i.e., the deconfinement phase. For finite lattice volume, the Polyakov line expectation value necessarily vanishes at $h = 0$ and is otherwise a smooth function of h. This is illustrated by curve (2) in figure 3, left panel. Only in the infinite volume limit, the $\langle P \rangle$ becomes a discontinuous function which approaches a finite value in the limit $h \to 0$ (see curve (3) in figure 3, left panel).

How can we anticipate the spontaneous breaking of the centre symmetry by means of a finite volume ergodic Monte-Carlo simulation?

10

A straightforward way is to study the gradient of $\langle P \rangle(h)$ at $h = 0$. This gradient should rise beyond bounds with increasing volume. Hence, we find

$$
\begin{aligned}
\frac{d\langle P \rangle(h)}{dh}\bigg|_{h=0} &= \lim_{h \to 0} \left[\left\langle P(0) \sum_{\boldsymbol{x}} P(\boldsymbol{x}) \right\rangle - \left\langle P(0) \right\rangle \left\langle \sum_{\boldsymbol{x}} P(\boldsymbol{x}) \right\rangle \right] \\
&= \left\langle P(0) \sum_{\boldsymbol{x}} P(\boldsymbol{x}) \right\rangle\bigg|_{h=0} \to \infty \ .
\end{aligned}
\tag{13}
$$

This agrees with the idea of ceasing centre sector transitions in the deconfinement phase (see (11)). Figure 3, right panel, shows the response function (13) for a $N^3 \times 4$ lattice as a function of β_{Wil} for several values of N. For this lattice geometry, the deconfinement phase is attained for $\beta \geq \beta_{\mathrm{dec}} \approx 2.3$. We observe that the response function is basically independent of the spatial size in the confinement phase for $\beta < \beta_{\mathrm{dec}}$ while it roughly scales with the volume in the gluonic plasma phase.

3   Fermi-Einstein condensation in the Schwinger model

It was already observed in [39] that centre sector transitions have far reaching phenomenological consequences for gauge theories with dynamical fermions at finite densities (such as QCD): for an even number of colours, the centre transformed background field can be viewed as imposing *periodic boundary conditions* for the matter fields. This opens the possibility that the centre dressed fermions undergo condensation similar to that which is known as Bose-Einstein condensation although the fermions are described by anti-commuting Grassmann fields. In analogy, this new phenomenon has been called *Fermi-Einstein condensation* [40]. For this scenario, centre transitions are essential hence relegating Fermi-Einstein condensation to the confining phase at intermediate values of the chemical potential. Consequently, Fermi-Einstein condensation evades the spin-statistic theorem since the fermion fields cannot be viewed as asymptotic states.

Here and in the next section, we further explore Fermi-Einstein condensation: (i) the U(1) gauge theory with fermions at finite densities, i.e., the Schwinger model, bears all prerequisites for Fermi-Einstein condensation. Because it can be solved analytically, it is also the ideal testbed to work out the consequences of the condensation. (ii) The rise of Fermi-Einstein condensation is QCD-like theories with an odd numbers of colours is less clear cut. We therefore investigate a QCD inspired SU(3) effective quark model to explore its possible existence and phenomenological consequences.

3.1   Schwinger-model essentials

Here we illustrate the role of the centre with the finite temperature Schwinger model in a spatial box of length L. The fermion field is anti-periodic and the gauge potential

periodic in Euclidean time with period $\beta = 1/T$. Only configurations with vanishing instanton number contribute to thermodynamic potentials such that we may assume that the fields are periodic in the spatial direction. Thus we consider the Schwinger model on the Euclidean torus $[0, \beta] \times [0, L]$ with volume $V = \beta L$. Only at the end of the calculation do we let the spatial extension L tend to infinity.

To continue we decompose the gauge potential as [29]

$$A_0 = \frac{2\pi}{\beta} h_0 + \partial_0 \lambda - \partial_1 \phi, \quad A_1 = \frac{2\pi}{L} h_1 + \partial_1 \lambda + \partial_0 \phi \qquad (14)$$

with constant toron fields h_0 and h_1. In the zero-instanton sector the mapping $\{h_\mu, \phi, \lambda\} \to A_\mu$ is one-to-one if we assume that the periodic functions λ and ϕ integrate to zero. Adding an integer either to h_0 or to h_1 is equivalent to performing a gauge transformation with winding and thus we must further assume that $0 \leq h_\mu < 1$. The Polyakov-line is given by

$$P(x_1) = \exp \left\{ i \int_0^\beta A_0 \, dx_0 \right\} = \exp\{2\pi i \, h_0\} \, \exp \left\{ -i\partial_1 \int_0^\beta \phi(x) \, dx_0 \right\} . \qquad (15)$$

Using the $[0, 1]$ periodicity of the partition function in h_0, the shift

$$h_0 \rightarrow h_0 + \alpha \qquad (16)$$

transforms the Polyakov line expectation value as

$$\langle P \rangle \rightarrow \exp\{2\pi i \, \alpha\} \langle P \rangle , \qquad \alpha \in [0, 1] \qquad (17)$$

and is identified as $U(1)$ centre transformation of the gauge fields. Hence, integration over the toron field h_0 implies an average over the centre sectors of the theory.

The Jacobian of the transformation (14) can be calculated by expanding all fields in Fourier modes and this way one finds [29]

$$\mathcal{D} A_\mu = (2\pi)^2 \det'(-\triangle) \mathcal{D}\phi \mathcal{D}\lambda \, dh_0 dh_1, \qquad (18)$$

where the primed determinant is the product of all *positive eigenvalues* of the operator $-\triangle$ on the torus. The functional integral over the gauge functions λ cancels out in expectation values for gauge invariant objects and the ϕ-dependence of the fermionic determinant can be calculated explictly by integrating the chiral anomaly [45]. The resulting functional integral over the periodic function ϕ (which must integrate to zero) is Gaussian and leads to the following expression for the grand canonical partition function $Z(\beta, L, \mu) = \text{tr} \left(e^{-\beta H + \mu N} \right)$:

$$Z(\beta, L, \mu) = (2\pi)^2 \sqrt{\frac{\det'(-\triangle)}{\det'(-\triangle + m_\gamma^2)}} \int_0^1 dh_0 \; z(h_0; \beta, L, \mu) \qquad (19)$$

$$z(h_0; \beta, L, \mu) = \int_0^1 dh_1 \; \det(i\slashed{\partial}_{h,\mu}) , \qquad (20)$$

12

where $m_\gamma = e/\sqrt{\pi}$ is the induced photon mass, and $z(h_0; \beta, L, \mu)$ is the *centre sector partition function* specified by a particular value of h_0. The Dirac operator is given by

$$i\partial\!\!\!/_{h,\mu} = i\partial\!\!\!/ - \left(\frac{2\pi}{\beta} h_0 - i\mu\right) \gamma^0 - \left(\frac{2\pi}{L} h_1\right) \gamma^1 . \tag{21}$$

The fermionic determinant $\det(i\partial\!\!\!/_{h,\mu})$ is an elliptic function of the constant toron fields h_0, h_1 and depends on the chemical potential. We use anti-periodic boundary conditions in time direction and periodic ones in spatial direction.

3.2 Centre-sector partition function

Let us further study the grand-canonical partition function $z(h_0; \beta, L, \mu)$ for a given centre sector. This study emulates the spontaneous breaking of centre symmetry where the theory is subjected to a "frozen" value of h_0. We stress that such the spontaneous breakdown cannot occur in 2 dimensions due to severe infra-red divergences induced by the would-be Goldstone bosons. We will however find that the suppression of centre sector transitions will lead to the wrong physics, and we believe that this is a generic truth valid also in higher dimensions.

To recover the familiar Fermi sphere physics, it is sufficient to consider large spatial volumes for the moment. In this limit, we will be able to analytically perform the integration over the spatial component h_1. To start with, we find:

$$\det(i\partial\!\!\!/_{h,\mu}) = e^{-\beta L f(\mu,\beta,L,h_0)} e^{-\beta E_{\text{Cas}}(L,h_1)} \tag{22}$$

where $E_{\text{Cas}}(L, h_1)$ is the μ independent Casimir energy (details of the calculation are left to appendix A):

$$E_{\text{Cas}} = -\frac{\pi}{6L} + \frac{\pi}{2L} (1 - 2h_1)^2 . \tag{23}$$

The μ and temperature dependence is encoded in the so-called 'free energy density'

$$f = -\frac{1}{L\beta} \sum_{n \in \mathbb{Z}} \ln\left[\left(1 + e^{2\pi i h_0} e^{-\beta(E_n+\mu)}\right) \left(1 + e^{-2\pi i h_0} e^{-\beta(E_n-\mu)}\right)\right] , \tag{24}$$

where $L E_n = 2\pi|n - h_1|$. For $L/\beta \to \infty$ the free energy density does not depend on the constant gauge field h_1. In a theory with *fixed* centre sector, i.e., with a *frozen value* h_0, the baryon number density would be given by

$$\rho_B = \frac{1}{L}\langle Q \rangle = -\frac{\partial f}{\partial \mu} \xrightarrow{L \to \infty} \frac{1}{\pi} \int_0^\infty dp \left\{ \frac{1}{e^{2\pi i h_0} e^{\beta(p-\mu)} + 1} - \frac{1}{e^{-2\pi i h_0} e^{\beta(p+\mu)} + 1} \right\} . \tag{25}$$

For the trivial centre sector $h_0 = 0$, we obtain the standard result of a free Fermi gas forming a Fermi sphere at finite values for μ. On the other hand, for the sector $h_0 = 1/2$, we obtain a scenario as if the fermions were to acquire Bose-statistics:

$$f(\mu, h_0 = 1/2) \xrightarrow{L \to \infty} -\frac{1}{\pi\beta} \int_0^\infty dp \left\{ \log\left(1 - e^{-\beta(p-\mu)}\right) + \log\left(1 - e^{-\beta(p+\mu)}\right) \right\} ,$$

Note that the latter free energy logarithmically diverges when $p \to \mu$. This is the usual instability due to condensation and corresponds to Fermi-Einstein condensation in the present context. Note that this singularity is integrable upon the integration over the centre sectors h_0.

In the remainder of this subsection, we will show that the assumption of a fixed centre sector will lead to the wrong physics in the case of the Schwinger model. The key observation is that the only excitations of the model are fermion anti-fermion bound states. The theory lacks any physical states which would couple to the chemical potential and would give rise to non-vanishing fermion density. The baryon density ought to vanish even in the case of non-vanishing values of the chemical potential. An inspection of (25) shows that this is not the case if we consider a fixed value of h_0 only. The momentum integral can be performed leaving us with ($T = 1/\beta$):

$$\pi \rho_B = \mu + T \left[\ln \left(1 + e^{-2\pi i h_0} e^{\mu/T} \right) - \ln \left(1 + e^{2\pi i h_0} e^{\mu/T} \right) \right], \qquad h_0 \neq 1/2. \qquad (26)$$

At $\mu = 0$, the contributions from fermions and anti-fermions to the baryon density cancels since there is no fermionic mass gap in the theory. For $h_0 = 1/2$, the theory produces a condensed states, and the result (26) cannot be extended to cover this case. For the trivial centre sector $h_0 = 0$, the baryon density linearly rises with the chemical potential. This is the well known Fermi-sphere behaviour for the 2-dimensional case. For any other value of h_0, the baryon density is complex which renders the findings difficult to interpret in physical terms.

The dependence of the baryon density on the chemical potential for a fixed centre sector is clearly spurious since the spectrum of the theory is free from states which carry baryon charge. A similar spurious dependence has been encounter in other theories as well which have been treated in an approximative way, and has been called the *silver blaze problem* [46].

3.3   Centre sector average

Considering individually the contributions of the centre sectors (specified by h_0) the free energy density has led to a singularity for $h_0 = 1/2$ associated with the condensation of fermions by virtue of periodic boundary conditions in this specific sector. In the Schwinger model, we are now in the comfortable situation that we can explore the physics of this Fermi-Einstein condensation since the centre sector average can be performed analytically. To this aim, we point out that the average of the fermion determinant over the spatial toron field can be written as (see appendix A.2 for details):

$$\int_0^1 dh_1 \, \det(i \partial\!\!\!/_{h,\mu}) = \frac{1}{\sqrt{2\tau} |\eta(i\tau)|^2} \sum_p e^{-\frac{1}{2}\pi\tau p^2 + 2\pi i p\gamma}, \qquad \gamma = h_0 + \frac{i\beta}{2\pi}\mu, \qquad (27)$$

where $\eta(i\tau)$ is the Dedekind eta-function (see (101)). The centre sector average, i.e., the integration over h_0, can be easily performed and restricts the Matsubara momentum sum

in (27) to the trivial momentum $p = 0$:

$$\int_0^1 dh_0 dh_1 \ \det(i\slashed{\partial}_{h,\mu}) \ = \ \sqrt{\frac{1}{2\tau} \frac{1}{|\eta(i\tau)|^2}} \ . \tag{28}$$

The Roberghe-Weiss symmetry for a model with global $U(1)$ centre-symmetry implies that the partition function can not depend on the imaginary part of μ. Analyticity suggests that this might also hold for real values of the chemical potential. Indeed for the present case, we find that any dependence on μ disappears after the integration over h_0.

From [47] we take the result

$$\det'^{1/2}(-\triangle) = \beta|\eta(i\tau)|^2 \tag{29}$$

to write

$$\int_0^1 dh_0 dh_1 \ \det(i\slashed{\partial}_{h,\mu}) \ = \ \sqrt{\frac{V}{2} \frac{1}{\det'^{1/2}(-\triangle)}}. \tag{30}$$

Inserting the latter finding into the grand canonical partition function (19), the square root of the determinant cancels, and we finally obtain

$$Z(\beta, L, \mu) \ = \ \sqrt{\frac{V}{2}} \frac{1}{\sqrt{\det'(-\triangle + m_\gamma^2)}} \ . \tag{31}$$

The key observation is that the μ dependence has disappeared implying that the centre sector average has solved the *silver blaze problem*: the baryon density vanishes independent of the value for the chemical potential as it should for the Schwinger model.

It is instructive for QCD model building to investigate how the centre sector average eliminates the μ-dependence. To this aim, we reconsider from the partition function (19) the factor

$$\int_0^1 dh_0 \ \det(i\slashed{\partial}_{h,\mu}) \ = \ e^{-\beta E_{\mathrm{Cas}}(L)} \int_0^1 dh_0 \prod_{n\in\mathbb{Z}} \left(1 + e^{2\pi ih_0}e^{-\beta(E_n+\mu)}\right)\left(1 + e^{-2\pi ih_0}e^{-\beta(E_n-\mu)}\right) \ , \tag{32}$$

where $L\,E_n = 2\pi|n - h_1|$. Expanding the product yields terms such as

$$\exp\{2\pi n\,ih_0\} \ \exp\{-\beta\,n\,\mu\} \ .$$

These terms vanish upon the integration over h_0 *unless* we have $n = 0$. Hence, the integral (32) does not depend on μ. This finding has a direct physical interpretation: $n = 0$ only occurs if as many fermions as anti-fermions contribute to the product. Hence, the h_0 integration eliminates all states which carry a net baryon charge thus solving the *silver blaze problem*.
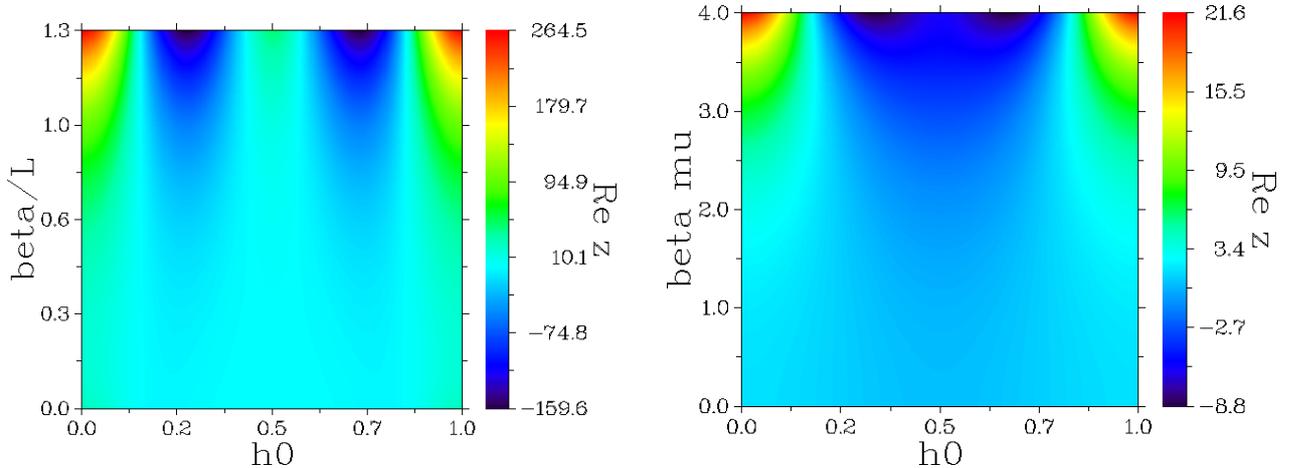
Figure 4: The real part of the differential contribution z in (20) to the fermion determinant as a function of h_0 and β/L for $\beta\mu = 4$ (left). The real part of z as a function of h_0 and $\beta\mu$ for $\beta/L = 1$ (right).

3.4 Volume studies

The question whether a particular centre sector is singled out or whether a more democratic average over the centre sectors is in order should be answered by the theory itself. For this investigation, we will here consider the large volume limits $L \to \infty$ and $\beta \to \infty$ and combinations of it.

In (19), we decomposed the grand canonical partition function Z into a part from dynamical fields and a part $z\left(h_0; \beta/L, \beta\mu\right)$ featuring the contributions from the toron fields. From the studies in the previous subsection, we already know that Z_{fer} is actually independent of $\beta\mu$. For a given value of the fugacity $\mu/T = \beta\mu$, we have calculated z as a function of h_0 and β/L. The colour coded result is shown in figure 4, left panel. The important observation is that the largest contribution arises from the trivial centre sector around $h_0 = 0$ at least for $\beta\mu > 1$ (note that the z is periodic, i.e., $z(h_0) = z(h_0) + n$, n integer). The maximum at $h_0 = 0$ even diverges in the limit $\beta/L \to \infty$.

Here is a lesson to learn if it comes to Monte-Carlo simulations. Assume that we were to estimate the h_0 integral using a Metropolis Monte-Carlo method. First of all we note that for $h_0 \neq \{0.5, 1\}$ the determinant is complex. For small enough $\beta\mu$, let us say $\beta\mu < 1$, we could use the real part of the determinant as a reweighting factor for the simulation. From figure 4, left panel, it is already clear that the method samples the region around $h_0 = 0$ to a large extent. For $\beta/L \gg 1$, other contributions from larger values of h_0 would be extremely rare. If we now stick to fixed aspect ratio β/L, we will find that for large values of $\beta\mu$ the real part of the determinant develops negative parts invalidating the Monte-Carlo approach altogether (see figure 4, right panel). The keypoint, however, is that the integral of z over h_0 yields a constant only dependent on the aspect ratio (see the
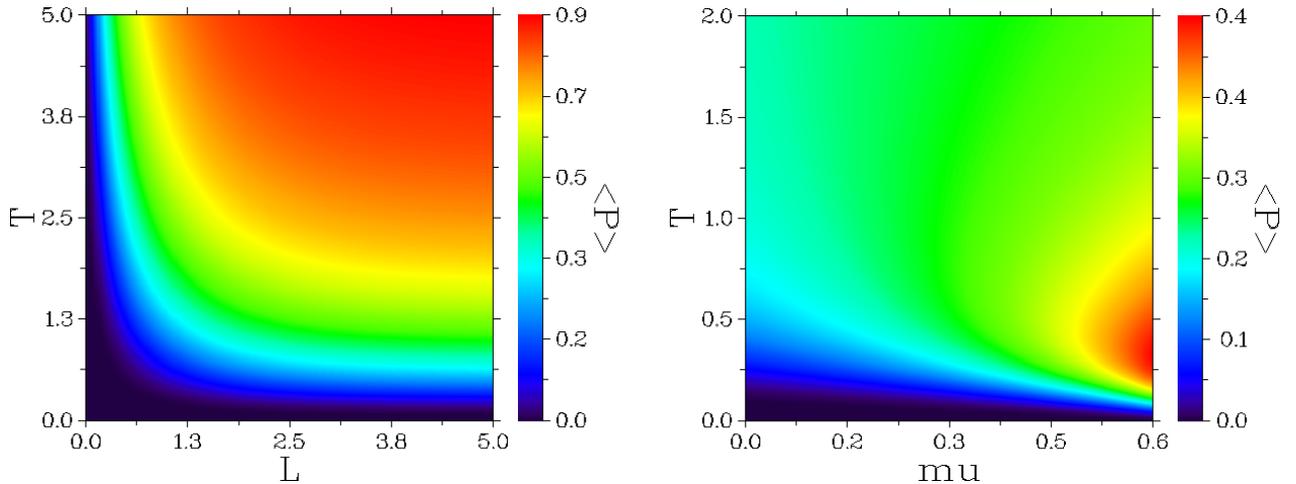
Figure 5: The Polyakov line expectation value for vanishing chemical potential as a function of the temperature T and spatial size L (left). $\langle P \rangle$ for a fixed aspect ratio $\beta/L = 1$ as a function of μ and T (right).

previous subsections). This means that integrating along the horizontal axis in figure 4, right panel, must produce the same value for every choice of $\beta\mu$. Obviously, sampling the whole range of h_0 values in the Monte-Carlo simulation is of key importance although difficult to achieve for $\beta/L \gg 1$, i.e., in the thermodynamic limit $L \to \infty$ with $T \neq 0$ fixed. Our findings suggest that the infinite volume zero-temperature limit of the QFTs (which we are going to discuss below) is delicate: we suggest that these limits should be taken at fixed aspect ratio $\tau = \beta/L$ and with one of the variables, L or β tending to infinity. In this context, the value $\tau = 1$ is of particular relevance for lattice gauge theories, since in this limit the rotational symmetry is recovered in the scaling limit of vanishing lattice spacing.

Although the centre transitions never cease in the Schwinger model, the trivial centre sector contributes an overwhelming part to the expectation values. This is also clear from the Polyakov line expectation value. This expectation value can be calculated in closed from for arbitrary lengths β, L and at presence of chemical potential μ (details of the calculation can be found in appendix A.3):

$$\langle P \rangle = e^{q\beta\mu} \exp\left(-\frac{\pi\beta m_\gamma}{4} \coth\left(\frac{m_\gamma L}{2} \right) \right) , \tag{33}$$

where $m_\gamma = e/\sqrt{\pi}$ is the dynamical generated photon mass which sets the scale of the theory.

Let us firstly discuss the case of vanishing chemical potential. Our findings for this case are summarised in figure 5, left panel. Note that the Polyakov line expectation value $\langle P \rangle$ always vanishes for any fixed spatial size L in the zero temperature limit $T \to 0$. On the other hand for a fixed temperature, $\langle P \rangle$ *increases* with increasing system size L, and

17

potentially approaches quite large value in the infinite volume limit:

$$\lim_{L \to \infty} \langle P \rangle \;=\; \exp\left\{ -\frac{\pi}{4} \frac{m_\gamma}{T} \right\} .$$

We will see below that this behaviour will be mirrored by the SU(2) Higgs theory.

Secondly, we consider the case of a non-vanishing chemical potential. For a fixed aspect ratio $\beta/L = 1$, figure 5, right panel, shows the Polyakov line expectation value as a function of μ and T. We point out that the fermion determinant is complex implying that the expectation value of a phase, in particular the Polyakov line, is not necessarily bounded anymore. These imaginary parts allow for the cancellations which are essential to solve the Silver Blaze problem and, at the same time, bear the potential for $|\langle P \rangle| \gg 1$. In the infinite volume limit, we now find

$$\lim_{L \to \infty} \langle P \rangle \;=\; \exp\left\{ \frac{\pi}{4} \frac{(\mu - m_\gamma)}{T} \right\} ,$$

which is bigger than one if the chemical potential exceeds the photon mass.

4 Fermi-Einstein condensation in a QCD quark model with confinement

4.1 Model building

In order to trace out the phenomenology of centre sector transitions and Fermi-Einstein condensation in a more QCD-type setting, we are here going to investigate an effective $SU(N_c = 3)$ quark theory in four dimensions. The so-called constituent quarks $q(x)$ satisfy the usual anti-periodic boundary conditions in Euclidean time direction (and periodic ones in the spatial directions)

$$q(x + \beta e_0) \;=\; (-1)\, q(x) , \qquad q(x + \beta e_k) \;=\; q(x), \qquad k = 1, 2, 3 . \tag{34}$$

The quarks possesses the constituent quark mass m and are assumed to only interact with an homogeneous temporal gauge field specifying the centre sector:

$$A_0^{(n)} = 2\pi n\, T\, H, \qquad 1 \le n \le N_c , \tag{35}$$

where the generator H is from the Cartan algebra, i.e., $H = \mathrm{diag}(1, \ldots, 1, 1 - N_c)/N_c$. The Polyakov line is in the centre of the group and the centre sector is labeled by n since the trace of the Polyakov line is given by

$$P \;=\; \frac{1}{N_c} \mathrm{tr}\, \exp\left\{ \mathrm{i} \int_0^\beta dx_0\, A_0^{(n)} \right\} \;=\; z_n, \qquad z_n \;=\; \exp\left\{ \frac{2\pi \mathrm{i}}{N_c} n \right\} . \tag{36}$$

The crucial observation [39] is that by means of a Roberghe-Weiss transformation quarks which are subjected to the background field $A_0^{(n)}$ can be considered as quarks manoeuvring in the trivial background $A_0^{(N_c)}$ but with changed boundary conditions:

$$A_0^{(n)}, \ q(x + \beta e_0) = -q(x) \qquad \leftrightarrow \qquad A_0^{(N_c)}, \ q(x + \beta e_0) = -z_n q(x) \ . \qquad (37)$$

For even N_c, there is the element $z_{N_c/2} = -1$, and it is this centre sector which is mapped to the trivial sector but with quarks now obeying *periodic* boundary conditions. Since it is essentially the boundary conditions which dictate the behaviour of the thermodynamical potentials, centre-dressed quarks follow Bose statistic and undergo condensation if the chemical potential approaches the fermionic mass gap [39]. Apparently, this scenario relies on the fact that (-1) is an element of the centre of the gauge group. This is only the case if the number of colours N_c is even. The more interesting, i.e., the more QCD type, case is $N_c = 3$ and evades the line of arguments. In this subsection, we will explore the phenomenology of the centre sector transitions in the realm of an effective quark model for $N_c = 3$.

The partition function of our model is given by

$$Z_Q \ = \ \sum_{n=1}^{N_c} \int \mathcal{D}q \mathcal{D}\bar{q} \ \exp\left\{\bar{q}\big(\mathrm{i}\slashed{\partial} + (A_0^{(n)} + \mathrm{i}\mu)\gamma^0 + \mathrm{i}m\big)q\right\} \ = \ \sum_{n=1}^{N_c} \mathrm{e}^{\Gamma^{(n)}}, \qquad (38)$$

$$\Gamma^{(n)} \ = \ \ln \det\left(\mathrm{i}\slashed{\partial} + (A_0^{(n)} + \mathrm{i}\mu)\gamma_0 + im\right) , \qquad (39)$$

where m is the quark mass and μ is quark chemical potential. The main difference to the model discussed in [39] is that we take into account that the gluonic sector is centre symmetric and the only centre sector bias arises from the quark determinant. Thus, the sum in (38) democraticly extends over all centre sectors without any further bias to the trivial centre sector.

4.2   Cold but dense matter

The calculation of determinant in (38) can be performed following the techniques developed for the Schwinger model. In 4 dimensions the determinant is more severe UV-divergent than in 2 dimensions but the *effective* theory only addresses the low-energy modes below a certain physical energy scale. In this approach, the cutoff scale Λ is finite and acquires a physical interpretation. Here, we are only considering temperatures which are small compared to this cutoff scale which allows us to effectively set $T/\Lambda \to 0$. Using a cutoff function provided by the Schwinger-proper time approach (see appendix A.1), we find:

$$\Gamma^{(n)} = \Gamma_0(\beta, L, \Lambda) \ + \ \Gamma_{\mathrm{den}}^{(n)}(\beta, L, \mu) \qquad (40)$$

with cutoff-dependent and cutoff-independent contributions

$$\Gamma_0(\beta, L, \Lambda) \;=\; \sqrt{\pi}\,\beta\Lambda\,\sum_p \left[1 - \mathrm{erf}\left(E(p)/\Lambda\right)\right] , \tag{41}$$

$$\Gamma_{\mathrm{den}}^{(n)}(\beta, L, \mu) \;=\; 2\sum_p \left\{ \ln\left(1 \,+\, z_n\,\mathrm{e}^{-\beta(E(p)+\mu)}\right) + \ln\left(1 + z_n^*\,\mathrm{e}^{-\beta(E(p)-\mu)}\right) \right\} , \tag{42}$$

where we have introduced the 1-particle energy by

$$E(p) \;=\; \sqrt{m^2 + p^2} , \qquad p \;=\; \frac{2\pi}{L}\,(n_1, n_2, n_3)^T , \quad n_k : \text{integer.} \tag{43}$$

The overall factor 2 in the 4-dimensional case (as compared to the 2d Schwinger model) arises from the two spin-orientations of the quarks. We point out that the cutoff dependent part Γ_0 is independent from the centre sector number n and the chemical potential while those parts $\Gamma_{\mathrm{den}}^{(n)}$ which do depend on μ and n are UV finite.

Let us now consider the case of low temperatures (and $\mu > 0$) for which we can neglect the anti-quark contributions to $\Gamma_{\mathrm{den}}^{(n)}$:

$$\beta m \gg 1 \qquad \Rightarrow \qquad \mathrm{e}^{-\beta(E(p)+\mu)} \to 0 . \tag{44}$$

For such low temperatures, even the mesonic type excitations can be neglected, and the partition function is approximately given by

$$Z_Q \;\approx\; \mathrm{e}^{\Gamma_0} \sum_{n=1}^{N_c} \prod_p \left[1 + z_n^*\,\mathrm{e}^{-\beta(E(p)-\mu)}\right]^2 . \tag{45}$$

Let us now specialise to $N_c = 3$, and expand the brackets. We obtain terms such as

$$[z_n^*]^\nu\,\mathrm{e}^{-\nu\,\beta(E(p)-\mu)} .$$

In order to evaluate the sum over the centre sectors, we use

$$\sum_{n=1}^3 z_n = 0 , \qquad \sum_{n=1}^3 z_n^2 = 0 , \qquad \frac{1}{3}\sum_{n=1}^3 z_n^3 = 1 .$$

Hence, the centre sector sum eliminates all coloured excitations from the partition function by projecting onto states with vanishing N-ality thus making manifest the confinement of colour. For $\mu < 6m$, we obtain the simple result

$$Z_Q \;\approx\; 3\,\mathrm{e}^{\Gamma_0}\left[1 \,+\, \sum_{p_1, p_2, p_3} \exp\left\{-\beta\left(E(p_1) + E(p_2) + E(p_3) - 3\mu\right)\right\}\right] , \tag{46}$$

where in the momentum sum only two of the three momentum can be equal. Since our model does not include any binding between the quarks, the sum $E(p_1) + E(p_2) + E(p_3)$

20
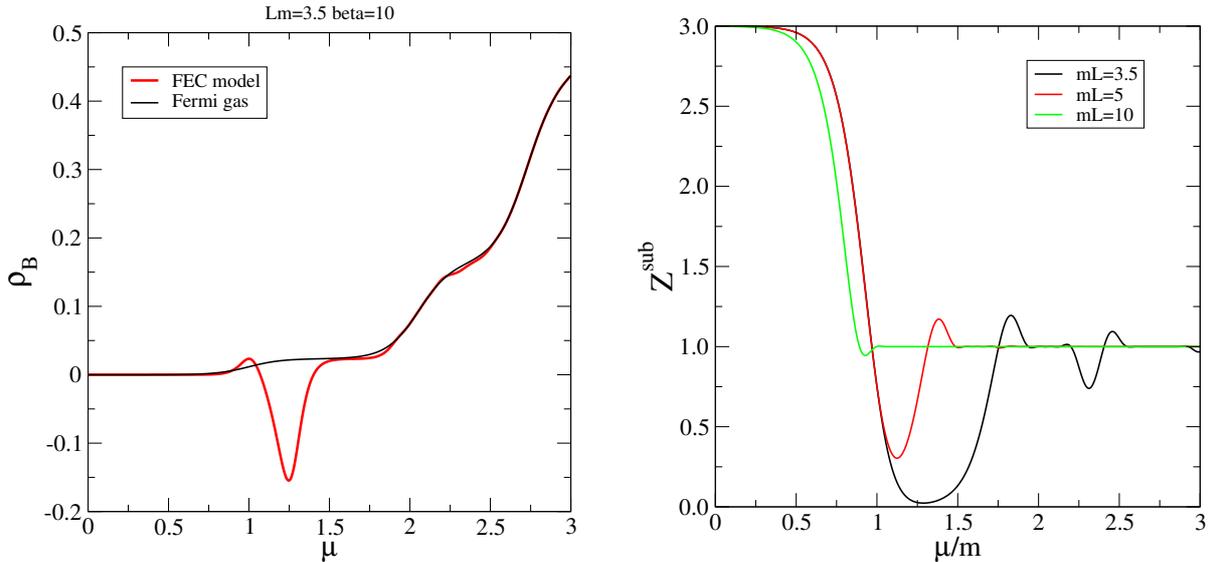
Figure 6: Baryon number as a function of the chemical potential for the confining quark model (FEC) in comparison to the standard Fermi gas result, left panel. The normalised partition function in (55), right panel.

can be interpreted as the energy of the "baryon" in the context of the present model. For chemical potentials smaller but close to the constituent quark mass m, the thermal energy density, i.e.,

$$E_{\text{therm}}(T) = -\frac{\partial \ln Z_Q}{\partial \beta} , \tag{47}$$

behaves like

$$E_{\text{therm}}(T) \approx 3m \exp\left\{-\frac{3(m - \mu)}{T}\right\}, \qquad \mu \lesssim m .$$

The first excitations in the model are baryonic ones. This result should be compared with the case of the "frozen" centre sector (which, in our simple case, is the free quark model):

$$E_{\text{therm}}^{\text{free}}(T) \approx m \exp\left\{-\frac{m - \mu}{T}\right\}, \qquad \mu \lesssim m .$$

Here, the mass gap is provided by the constituent quark mass, and the first excitations which are encountered by increasing the temperature stating at $T = 0$ are quark excitations. As in the Schwinger-model, the centre sector sum solves the Silver-Blaze problem.

4.3 Condensation of centre dressed quarks

The thermodynamical quantities of the present quark model can also be calculated exactly by evaluating e.g. (42) by numerical means. The constituent quark mass m here sets the fundamental energy scale. It turns out that the approximations leading to (46) are only

valid for rather low temperatures, i.e., $\beta m \approx 100$. In this subsection, we study intermediate temperatures and several spatial extensions such as

$$\beta m \;=\; 10\,, \qquad L\,m \;=\; 3\ldots 10\,. \tag{48}$$

We are interested in the baryon number Q_B which is accessible by

$$Q_B \;=\; T\,\frac{\partial \ln Z_Q}{\partial \mu} \;=\; \sum_n \omega_n \sum_p \left[\frac{z_n^*}{e^{\beta(E(p)-\mu)} + z_n^*} - \frac{z_n}{e^{\beta(E(p)+\mu)} + z_n} \right]\,, \tag{49}$$

where the centre sector weights are given by

$$\omega_n \;=\; \frac{\exp\{\Gamma_{\mathrm{den}}^{(n)}\}}{\sum_n \exp\{\Gamma_{\mathrm{den}}^{(n)}\}}\,. \tag{50}$$

Note that for $\mu \neq 0$ the weights can be complex and therefore evade a straightforward interpretation as probabilistic weight for a given centre sector. An inspection of (42) shows that

$$\omega_1 \;=\; \omega_2^*\,, \qquad \omega_3 \in \mathbb{R}\,, \qquad \sum_n \exp\{\Gamma_{\mathrm{den}}^{(n)}\} \in \mathbb{R}\,. \tag{51}$$

We can always compare our findings with those from a free Fermi gas model for which we have

$$\omega_1 \;=\; 0\,, \qquad \omega_2 \;=\; 0\,, \qquad \omega_3 \;=\; 1 \qquad \text{(Fermi gas)}\,. \tag{52}$$

The calculation of the centre sector weights is delicate since the effective actions Γ_n generically are large numbers. To facilitate this calculation, we introduce the subtracted actions by

$$\bar{\Gamma}_n \;=\; \Gamma_n - \Gamma_{\mathrm{max}}, \qquad \Gamma_{\mathrm{max}} \;=\; \max\left(\mathrm{Re}\,\Gamma_n\right) \quad \forall n\,. \tag{53}$$

It is easy to check that the centre sector weights are actually independent of this shift:

$$\omega_n \;=\; \frac{\exp\{\Gamma_{\mathrm{den}}^{(n)}\}}{\sum_n \exp\{\Gamma_{\mathrm{den}}^{(n)}\}} \;=\; \frac{\exp\{\bar{\Gamma}_{\mathrm{den}}^{(n)}\}}{\sum_n \exp\{\bar{\Gamma}_{\mathrm{den}}^{(n)}\}}\,. \tag{54}$$

Figure 6, left panel, shows our finding for the Baryon density as a function of the chemical potential μ for a *small* spatial volume:

$$m\,L \;=\; 3.5\,.$$

For $\mu/m \approx 1.3$, we observe that the baryon density strongly peaks for the FEC model. This peak is absent in the standard Fermi gas model. The reason for this peak are cancellations between the centre sector which nullify the partition function. To see this, we introduce the normalised partition function by

$$Z^{\mathrm{sub}} \;=\; \exp\{\Gamma_n\}\,e^{-\Gamma_{\mathrm{max}}} \;=\; \sum_n \exp\{\bar{\Gamma}_{\mathrm{den}}^{(n)}\}\,. \tag{55}$$
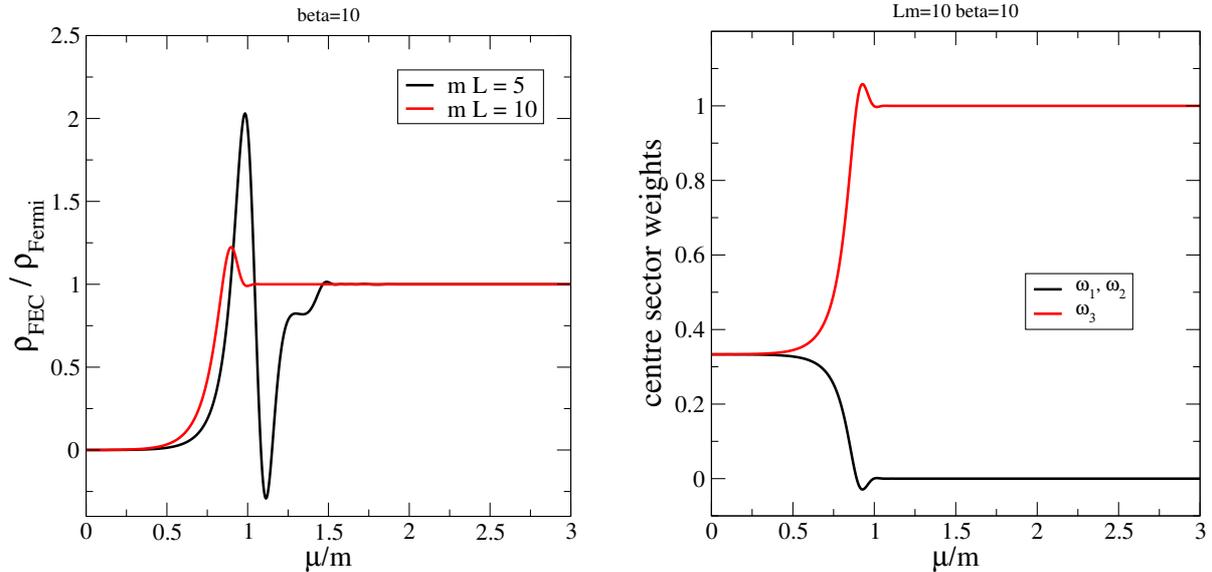
Figure 7: Ratio between the baryon density of the FEC model and that of the standard Fermi gas model for two spatial sizes L, left panel. The real part of the centre sector weights $\omega_{1\ldots3}$, right panel.

Note that $\Gamma_{\max} \in \mathbb{R}$ implying that a *zero* of Z^{sub} goes along with a *zero* of the full partition function Z_Q. The quantity Z^{sub} also appears in the denominator of the sector weights ω_i. Figure 6, right panel, shows the normalised partition function Z^{sub} as a function μ. We observe for $mL = 3.5$ that Z^{sub} almost vanishes for the chemical potential corresponding to the peak position in the baryon density. Increasing the spatial size, we find the near-zero regime of Z^{sub} is lifted and the peak of the baryon density diminished. For an even number of colours, the rise of the baryon number due to a vanishing partition function was called *Fermi-Einstein condensation* (FEC) [39, 40]. For small enough spatial size, we observe that FEC can also occur for an odd number of colours and thus in QCD-like theories.

Let us now study the baryon density for the bigger systems with $mL = 5$ and $mL = 10$. Figure 7, left panel, shows the baryon density of the FEC model normalised to that of the Fermi gas model. We observe that for small values of μ the baryon density is suppressed compared to that from the Fermi gas model. For $mL = 10$, this suppression ceases for $\mu/m \approx 0.9$ and the FEC baryon density equals that of the Fermi gas model. We see here confinement at work: while in the Fermi gas model, the baryon density rises with increasing μ by exciting single quarks into the system. In the FEC model at small values of μ, the only way to increase the baryon density is to excite a baryon with mass $3m$ (in our model). For $\mu \approx 0.9m$, deconfinement sets in and density rises further on by adding quarks to the system. This interpretation is corroborated by an inspection of the centre sector weights ω_i in figure 7, right panel. Note that ω_3 corresponds to the trivial centre sector ($z_3 = 1$). For small values of μ, the real part of the weights are roughly the same and equal $\approx 1/3$. This indicates that centre sector transitions frequently occur wiping coloured states from the

23
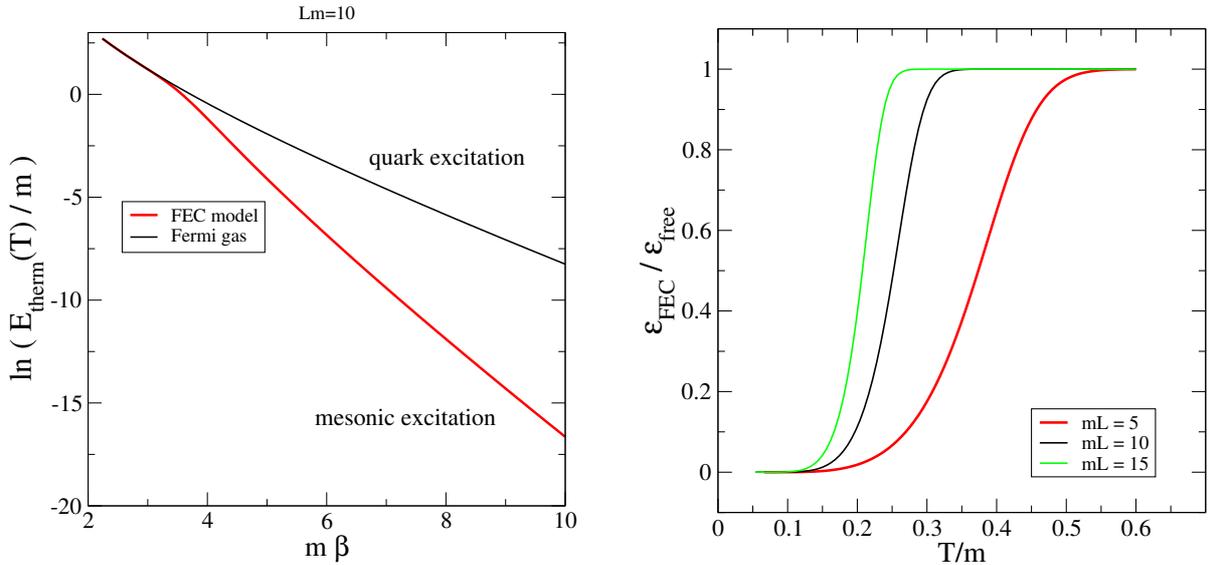
Figure 8: Thermal energy $E(T)$ as a function of the inverse temperature β for the FEC model and the free Fermi gas (left). Ratio between the thermal energy densities of the FEC model and the free Fermi gas (right).

partition function thus installing confinement. For $\mu > 0.9m$, the weights of the non-trivial centre sectors, i.e., $\omega_{1,2}$, vanish and only the trivial centre sector significantly contributes. Hence, the FEC model migrates into the Fermi gas model.

4.4 Deconfinement at finite temperatures

Let us now focus on the case of vanishing chemical potential, i.e., $\mu = 0$. Our aim here will be to explore the phenomenology of the centre sector transitions far from the dense regime. The quantity of main interest is the thermal energy density $E_{\text{therm}}(T)$ in (47). In the FEC quark model, we obtain:

$$
E_{\text{therm}}(T) \;\; = \;\; \sum_n \omega_n \sum_p E(p) \left[\frac{z_n^*}{e^{\beta E(p)} + z_n^*} \;\; + \;\; \frac{z_n}{e^{\beta E(p)} + z_n} \right] \; . \tag{56}
$$

The centre sector partition functions $\Gamma_{\text{den}}^{(n)}(\beta, L, \mu = 0)$ are real and positive functions of the temperature $T = 1/\beta$. The centre sector weights ω_i, $i = 1 \ldots 3$ satisfy

$$
\omega_i \in \mathbb{R}, \qquad \omega_i \geq 0, \qquad \sum_{i=1}^{3} \omega_i \;\; = \;\; 1 \; , \tag{57}
$$

and, thus, can be interpreted as the probability with which each sector contributes to e.g. the thermal energy in (56). For later reference, we also quote the thermal energy of a

24
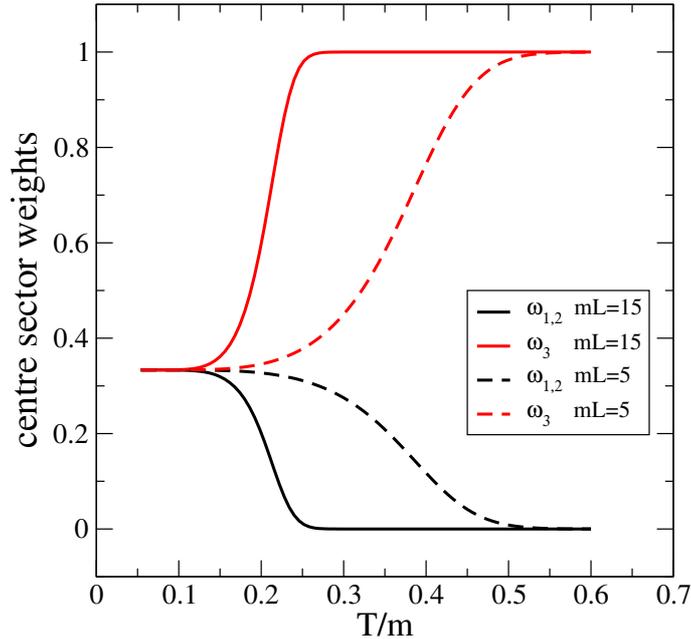
Figure 9: Probabilistic weights for the realisation of the centre sector n.

free Fermi gas:

$$E_{\text{therm}}^{\text{free}}(T) \;\; = \;\; 2 \sum_p E(p) \, \frac{1}{e^{\beta E(p)} + 1} \; . \tag{58}$$

Note that antiquarks contribute in the same way as quarks. Hence, the factor 2 in (58).

For first insights, we consider the case of small temperatures:

$$\beta \, m \; \ll \; 1 \; .$$

The partition function (38) can then be approximated by

$$Z_Q \;\; = \;\; e^{\Gamma_0} \sum_{n=1}^{N_c} \prod_p \left[1 + z_n^* \, e^{-\beta E(p)} \right]^2 \left[1 + z_n \, e^{-\beta E(p)} \right]^2 \tag{59}$$

$$\approx \;\; 3 \, e^{\Gamma_0} \left[1 + 2 \sum_p e^{-\beta \, 2 \, E(p)} \right] . \tag{60}$$

For $\mu = 0$, the most important contribution to the low temperature partition function arises from mesonic states. Figure 8, left panel, shows the thermal energy for the FEC model in comparison to the free Fermi gas. At large β (low temperatures), the FEC thermal energy is suppressed like $\exp\{-\beta \, 2m\}$ since only mesonic excitations are possible by virtue of confinement. This is in contrast to the free Fermi gas where the contribution from single quark states yields a suppression only of order $\exp\{-\beta \, m\}$.

25
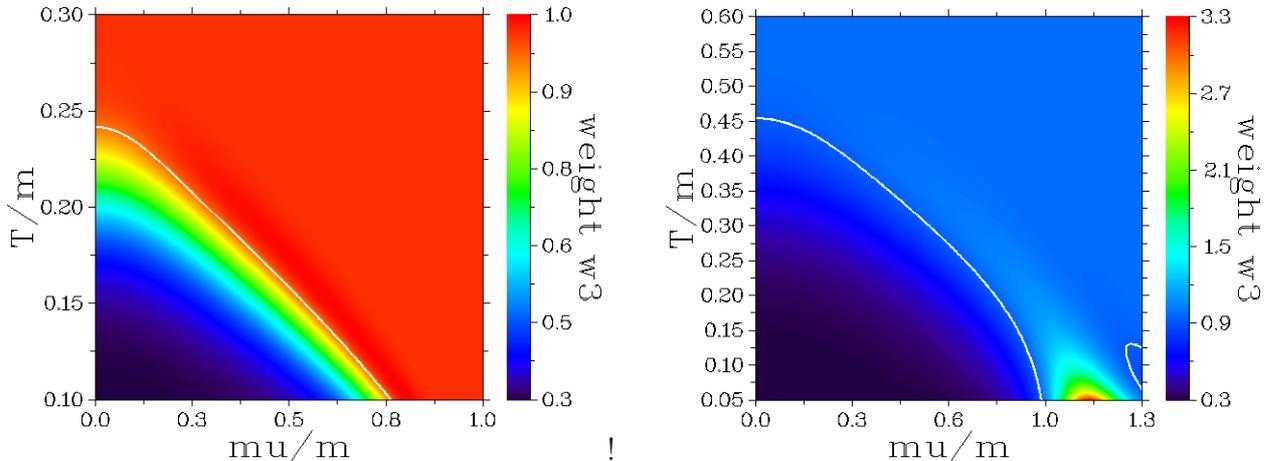
Figure 10: Phase diagram of the FEC model as shown by the centre weight ω_3. Left: large volumes, i.e., $mL = 15$. Right: small volumes, i.e., $mL = 5$. The contours correspond to $\omega_3 = 0.95$.

Dividing the thermal energy by the spatial volume yields the thermal energy density:

$$\epsilon_{\text{FEC}} = E_{\text{therm}}/L^3, \qquad \epsilon_{\text{free}} = E_{\text{therm}}^{\text{free}}/L^3.$$

Figure 8, right panel, shows the ratio of thermal energy densities of the FEC model and the free Fermi gas. Around $T \approx 0.2$, we observe that the FEC energy density rapidly approaches that of the Fermi gas. We attribute this behaviour to a deconfinement phase transition. Indeed, figure 9 shows the centre sector weights ω_i. For small temperatures $T \ll m$, we observe that all weights roughly equal $1/3$ indicating an equal contribution from the centre sectors to thermodynamical quantities. For $T > 0.2m$, we find that the non-trivial centre sectors cease to contribute implying that the FEC model turns into the free Fermi gas theory at high temperatures.

4.5   The phase diagram from confinement

We are now considering both finite temperatures as well as a non-vanishing chemical potential. In order to trace out the phase diagram, we will employ the centre weight $\omega_3 \in \mathbb{R}$: for a vanishing chemical potential, all weights ω_i are real numbers which sum to unity. At high temperatures, we have observed in the previous subsection that $\omega_3 \to 1$ while $\omega_{1,2} \to 0$ thus showing confinement. For large non-vanishing chemical potentials, the latter is still true: ω_3 close to 1 signals the transition of the FEC model to the free Fermi gas. Thus, an inspection of $\omega_3(\mu, T)$ maps out the deconfinement region in the phase diagram.

Note that the $\omega_3 \leq 1$ only strictly holds for $\mu = 0$ where the weights ω_i enjoy an interpretation as probabilities. Though in the deconfinement regime ω_3 will approach 1, there is no need for $\mu \neq 0$ that ω_3 is bounded from above by 1. In fact, we have seen for small spatial

extensions $mL \lesssim 2.5$ that Fermi-Einstein condensation occurs with potentially large values of ω_3 (see figure 7).

Figure 10 shows our colour coded result for $\omega_3(\mu, T)$. In the large volume limit, e.g. for $mL = 15$, the result is as expected: there is quite a sharp transition between the hadronic regime at low μ and T to the deconfinement regime under extreme conditions. For a smaller volume, e.g. $mL = 5$ (right panel), large values of ω_3 can be observed for low temperatures and μ close to the mass threshold. This is the regime for which the partition function cancels to a large extent due to centre sector transitions.

5 Centre sector transitions in the gauged Ising model

Above using the Schwinger model as well as a SU(3) effective quark theory, we have stressed the phenomenological importance of transitions between the centre sectors of the theory under investigations. It remains to show that these centre transitions do occur if dynamical matter is present: since this matter explicitly breaks centre symmetry, transitions between centre sectors could be prohibited in the infinite volume limit. With "matter", we here address any dynamical fields (in addition to the Yang-Mills gauge fields) which transform under the fundamental representation of the gauge group. An important example is the theory of strong interactions, QCD, which is an $SU(3)$ Yang-Mills theory with e.g. three (light) flavours of quark matter.

In the remainder of the paper, we discuss theories at zero chemical potential and search for potential transitions between the centre sectors. Since the Schwinger model does not possess genuine phase transitions due to its 2-dimensional nature, we start the considerations with the $\mathbb{Z}_2$ gauge theory coupled to Ising matter in 3-dimensions. This theory is easily accessible by means of Monte-Carlo simulations, and offers the possibility of phase transitions. We will focus on two competing scenarios which both sketch a different picture of the realisation of the centre symmetry:

(i) The explicit breaking triggers a spontaneous breakdown of centre symmetry. Centre sector tunneling does not take place. Observables only receive contributions from the trivial centre sector.

(ii) The explicit breaking of centre symmetry breaking does not bring an end to the centre sector transitions. Observables are still averaged over the different sectors. There is, however, a bias towards the trivial sector.

Note that, in scenario (ii), the matter sector is a correction to the gauge sector of pure Yang-Mills theory. The Polyakov line expectation value is only non-zero since the lattice configurations are biased towards the trivial centre sector. Centre symmetry does also break spontaneously at high temperatures though the critical temperature can be quantitatively

different from the pure Yang-Mills case. Note that the idea of a spontaneously broken symmetry which is also explicitly broken is a useful concept: in QCD, chiral symmetry is explicit broken by the current quark masses. Additional spontaneous chiral symmetry breaking assigns the pions the role of "almost" Goldstone bosons and explains their particular role in the hadron spectrum.

5.1 Phase diagram of the gauged Ising model

We are here going to discuss the $\mathbb{Z}_2$-gauge theory minimally coupled to Ising spins $\sigma_x \in \{\pm 1\}$ to ensure $\mathbb{Z}_2$ gauge invariance. The model has been considered as the most simple gauged Higgs theory, and it has been shown that its phase diagram has the same qualitative features than e.g. the SU(2)-Higgs theory [48–52]. As familiar from lattice Yang-Mills theories, the gauge fields are represented by the links $Z_\mu(x) \in \{\pm 1\}$. The partition function of the theory is given by

$$Z = \int \mathcal{D}Z_\mu \, \mathcal{D}\sigma \, \exp\{S_Z\}, \tag{61}$$

$$S_Z = \beta_{\mathrm{I}} \sum_{x, \mu > \nu} P_{\mu\nu}(x) \, + \, \kappa \sum_{x \, \mu} \sigma_x Z_\mu(x) \, \sigma_{x+\mu} \,, \tag{62}$$

where $P_{\mu\nu}(x)$ is the usual plaquette

$$P_{\mu\nu}(x) = Z_\mu(x) \, Z_\nu(x + \mu) \, Z_\mu(x + \nu) \, Z_\nu(x) \,. \tag{63}$$

One easily verifies the invariance of the partition function under gauge transformations ($\Omega_x \in \{\pm 1\}$):

$$\sigma \to \sigma_x^\Omega = \Omega(x) \, \sigma_x, \qquad Z_\mu(x) \to Z_\mu^\Omega(x) = \Omega(x) \, Z_\mu(x) \, \Omega(x + \mu) \,. \tag{64}$$

For $\kappa = 0$, the Ising matter decouples from the gauge sector, and we are dealing with a pure $\mathbb{Z}_2$ gauge theory. It is well known that this theory confines static centre charges, and the static potential between two static charges is linearly rising with their distance. The Polyakov lines is an order parameter for confinement. For non-vanishing but small values κ, the dynamical Ising spins can screen the static centre charges, and we obtain *string breaking*: the linearly rising static potential at large distances flattens when the potential energy is sufficient to create a dynamical matter pair. Hence, the phase diagram as a function of κ and β_{I} is expected to show the same features as that of the SU(2) Higgs theory.

Figure 11, left panel, summarises this diagram: due to the lack of a local order parameter, a cross-over region from the string breaking regime to the so-called Higgs phase is expected. We verified these expectations by calculating Polyakov line expectation values using a 20^3 lattice. Both, the update of the links $Z_\mu(x)$ and the matter fields σ_x have been done by standard heat bath techniques. We calculated the Polyakov expectation value for 204×201 different values in the β_{I}-κ plane. Our numerical findings are colour-coded and summarised in figure 11, right panel. Both, the cross-over regime as well as the finite size transition is clearly visible.
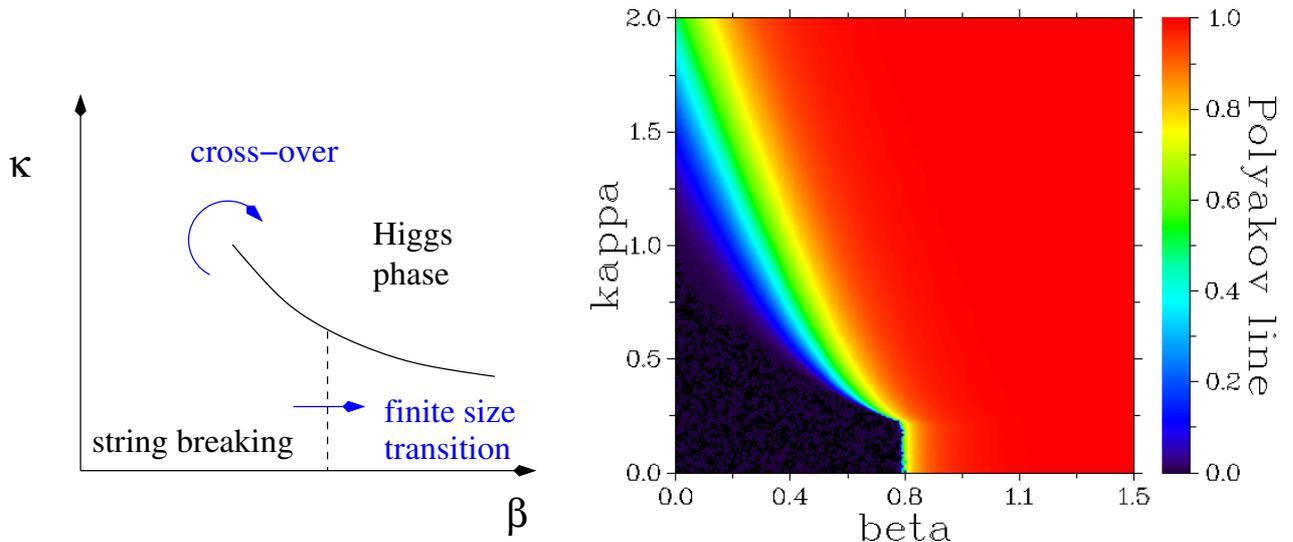
Figure 11: Sketch of the phase diagram (left); Polyakov line expectation value of the gauged Ising model as function of $\beta_{\rm I}$ and κ.

5.2 The interface tension of the trivial centre sector

Let us briefly discuss the "empty" vacuum of the gauged Ising model. The discussion in the context of pure Yang-Mills theory in subsection 2.1 can be straightforwardly transferred to the case of the $\mathbb{Z}_2$ gauge theory: The gauge inequivalent empty vacua are characterised by the values of the homogeneous Polyakov lines in each direction. Thus each of the Polyakov lines P_1, P_2 and P_3 takes values ± 1, there are $2^3 = 8$ states which we need to consider. The $\mathbb{Z}_2$ *centre transformation*

$$Z_\nu(x) \to (-1)\, Z_\nu(x) \qquad \forall \ \ x_\mu,\ \mu \neq \nu, \qquad x_\nu \ \text{fixed} \tag{65}$$

is discrete, changes the sign of the Polyakov line P_ν and therefore maps one empty vacuum state to another.

Before we proceed to consider the centre sector transitions within the gauged Ising model, we here discuss centre interfaces in the particular sector with all Polyakov lines trivial. For this "empty" vacuum state a gauge can be found where all links are one:

$$(P_1, P_2, P_3) \ = \ (1, 1, 1)\,, \qquad Z_\mu(x) = 1 \ \ \forall \ x,\ \mu\,. \tag{66}$$

The gauged Ising model then collapses to the standard Ising model with ferromagnetic bonds only.

If $|\psi\rangle$ is particular 2d array of spin at $x_0 = 0$, i.e., the so-called *in*-state and if $|^z\psi\rangle$ is a centre copy of this state for which all spin are reflected, we would like to investigate the overlap of the true vacuum state $|\psi_0\rangle$ with either $|\psi\rangle$ *and* $|^z\psi\rangle$. If centre symmetry is realised in the Wigner mode, the vacuum is centre symmetric yielding an overlap in both

29
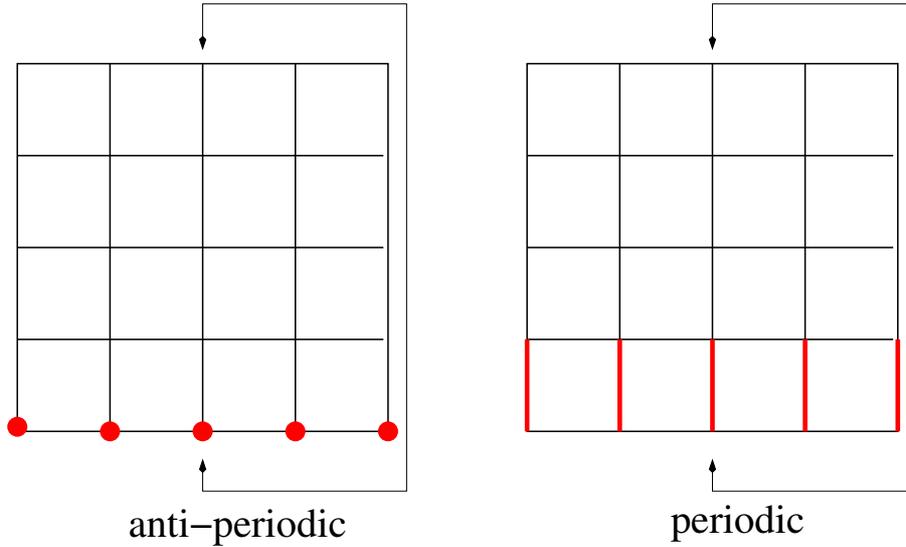
Figure 12: Partition function with anti-periodic boundary conditions rewritten as a partition function with a centre twist.

cases. If the centre symmetry is spontaneously broken, the overlap vanishes for one of the matrix elements. To investigate the spontaneous breaking of centre symmetry, we thus study:

$$\chi = \frac{\langle {}^z\psi | \exp\{-H/T\} | \psi \rangle}{\langle \psi | \exp\{-H/T\} | \psi \rangle} , \tag{67}$$

where H is the Hamilton operator and T is the temperature. For sufficiently small temperatures, the exponentials in the latter equation project onto the ground state $|\psi_0\rangle$, and we obtain:

$$\chi \rightarrow \frac{\langle {}^z\psi | \psi_0 \rangle \langle \psi_0 | \psi \rangle}{|\langle \psi_0 | \psi \rangle|^2} = \begin{cases} 1 & \text{Wigner-Weyl realisation} \\ 0 & \text{spontaneous symmetry breaking.} \end{cases} \tag{68}$$

In the functional integral approach, χ is given by the ratio of two partition function: the partition function with the spins σ_x obeying *anti-periodic* boundary conditions constitutes the numerator in (67), while the standard partition function with period spins is in the denominator. A connection to the centre symmetry can be established by "pushing out" the centre element to the links:

$$ {}^z\sigma_x \, U_\mu(x) \, \sigma_{x+\mu} = \sigma_x \, (-1) \, U_\mu(x) \, \sigma_{x+\mu} . $$

The net effect is illustrated in figure 12:

$$\chi = \frac{Z_{\text{anti-periodic}}}{Z_{\text{periodic}}} = \frac{Z_{\text{twist}}}{Z_{\text{periodic}}} . \tag{69}$$

30

We expect that the transition between centre sectors are exponentially suppressed with a slope given by the size of the centre interface. For a $N^2 \times N_t$ lattice, the minimal surface of the centre interface is N^2. It is therefore convenient to introduce the interface tension σ by

$$\chi = \exp\left\{ - N^2 \, \sigma(\kappa) \right\}. \tag{70}$$

For small values κ, χ can be directly calculated by the so-called strong coupling expansion, i.e., the Taylor expansion with respect to κ. For large values of κ, χ can be obtained by means of a duality transformation. In 3d Ising model is dual to the 3d $\mathbb{Z}_2$ gauge theory, and χ appears to be the $\mathbb{Z}_2$ expectation value of the maximal spatial Wilson loop (details will be presented elsewhere). Altogether, we find:

$$\sigma(\kappa) \approx \begin{cases} \kappa^{N_t} & \text{for} \quad \kappa \ll 1 , \\ 2\kappa & \text{for} \quad \kappa \gg 1 . \end{cases} \tag{71}$$

For a fixed aspect ratio N_t/N and in the thermodynamic limit $N \to \infty$, we find that the theory is in the disordered phase for small κ, i.e., $\chi \to 1$, implying that centre sector transitions do occur frequently. For large κ, the interface tension is independent of N_t and large showing that spontaneous centre symmetry breaking occurs in this case.

For intermediate values of κ the interface tension must be obtained by numerical means. The ratio of partition functions, i.e., χ, can be numerically calculated in an efficient way using the so-called *snake-algorithm* [53]. Our numerical results are shown in figure 13. In the ordered phase at $\kappa = 0.20$, we observe an exponential decrease of the interface tension σ with N in line with result from the leading order Taylor expansion in κ. For the ordered phase at $\kappa = 0.25$, we confirm that the interface tension is indeed independent of the volume.

5.3 Centre sectors and parametric transition

While in the previous subsection, the link variables have been frozen to the trivial centre sector, we now consider the transition element χ of the gauged Ising model where all links $Z_\mu(x)$ are dynamical. Defining the twisted link variables by

$$\begin{align} Z_3^{\text{twist}}(x) &= (-1)Z_3(x) \qquad \forall x_1, x_2; \quad x_3 \ \text{fixed} , \tag{72} \\ Z_\mu^{\text{twist}}(x) &= Z_\mu(x) \qquad\qquad \text{else,} \end{align}$$

the partition function of the twisted partition function is given by

$$Z_{\text{twist}} = \int \mathcal{D}Z_\mu \, \mathcal{D}\sigma \, \exp\{S_Z\}, \tag{73}$$

$$S_Z = \beta_{\text{I}} \sum_{x,\mu>\nu} P_{\mu\nu}[Z] + \kappa \sum_{x,\mu} \sigma_x Z_\mu^{\text{twist}}(x) \, \sigma_{x+\mu} . \tag{74}$$

Given the invariance of the measure and of the plaquette,

$$\mathcal{D}Z_\mu = \mathcal{D}Z_\mu^{\text{twist}} , \qquad P_{\mu\nu}[Z] = P_{\mu\nu}[Z^{\text{twist}}] ,$$
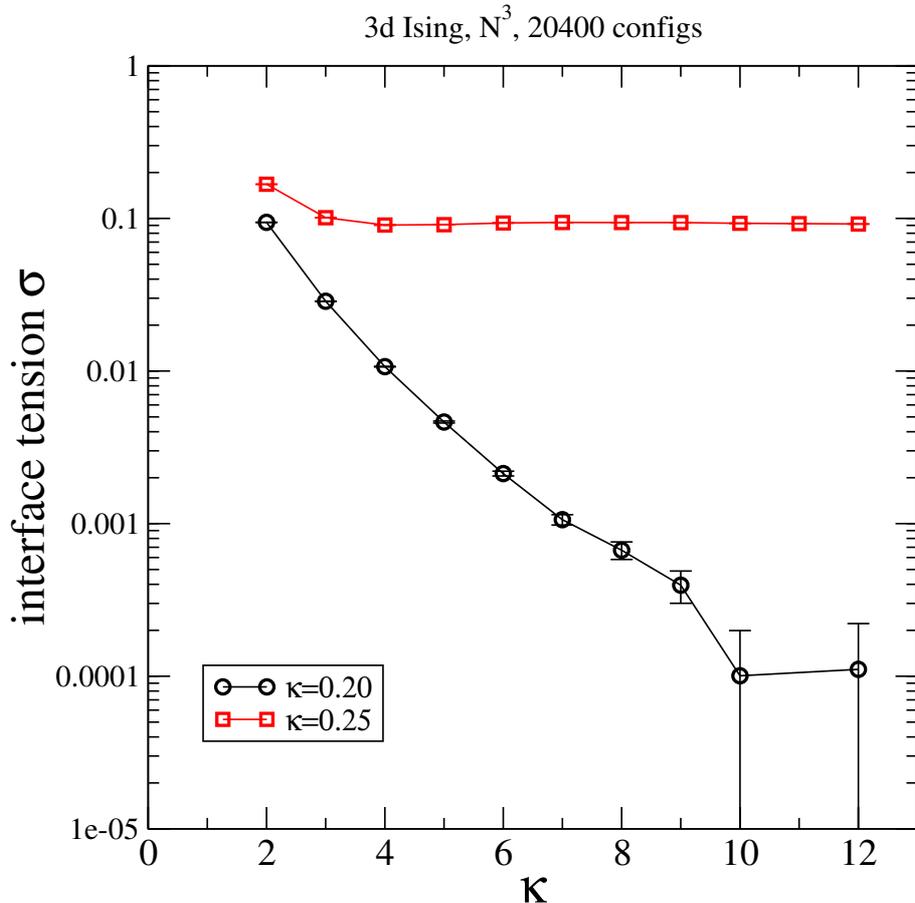
Figure 13: The interface tension of the 3d Ising model as a function of the system size N for interaction strength $\kappa = 0.20$ (disordered phase) and $\kappa = 0.25$ (ordered phase).

one easily obtains

$$Z_{\text{twist}} = Z_{\text{periodic}} \quad \Rightarrow \quad \chi = 1 . \tag{75}$$

In the gauged Ising model (as well as in the Schwinger model and QCD), the centre twist is part of the gauge field average. It is therefore, strictly speaking, impossible to consider a spontaneous breakdown of the centre symmetry. Note, however, that the matter fields break the centre symmetry *explicitly*. Depending on the coupling strength κ and the temperature, N_t respectively, this explicit breaking can be small. Actually for small κ, we are going to show that at low temperatures the explicit breaking is rather irrelevant while above a critical value for the temperature, the explicit breaking is strong in the sense that it does not makes sense to even consider an approximate centre symmetry. We call this a *parametric transition.*

Let us firstly illustrate the explicit breaking in the gauged Ising model. To this aim, we integrate over the Ising spin σ_x for a given link distribution $Z_\mu(x)$. The resulting
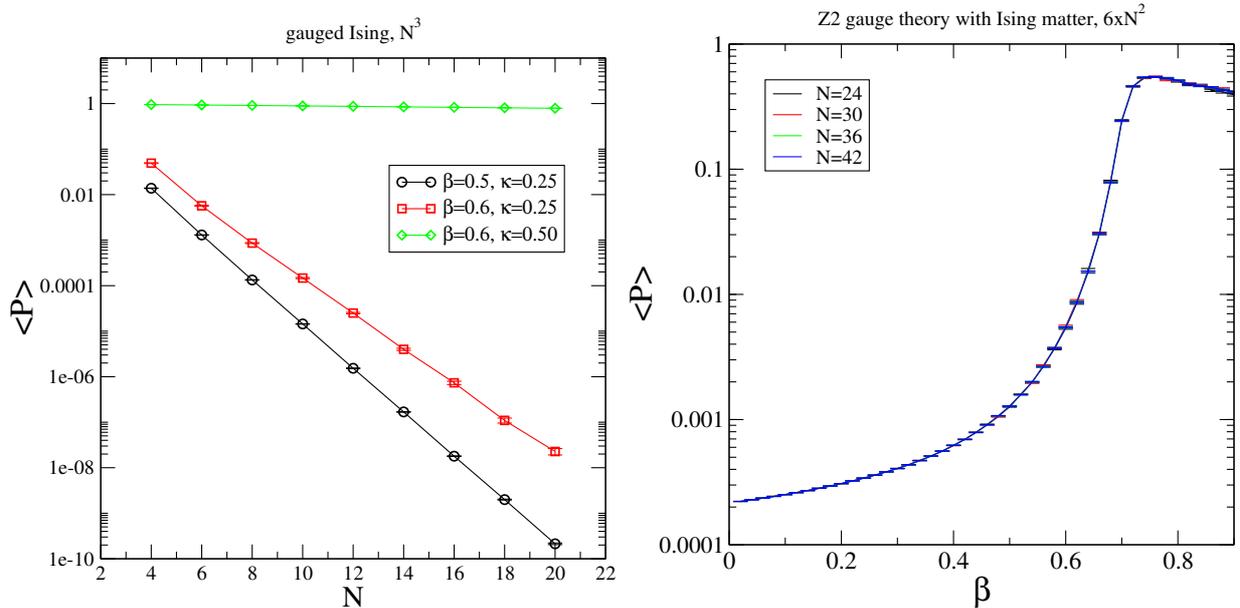
Figure 14: Polyakov line expectation values of the gauged N^3 Ising model as a function of the system size N (left). Same quantity for a $6 \times N^2$ lattice as a function of β_{I} (right).

probabilistic factor contains contractible Wilson loops $W[Z]$ as well as the Polyakov line $P[Z]$ (for simplicity we here consider infinite space)

$$\int \mathcal{D}\sigma \, \exp\{S_Z[Z]\} \;=\; \sum_{\mathcal{C}} \kappa^{L(\mathcal{C})} \, W_{\mathcal{C}}[Z] \;+\; \kappa^{N_t} \sum_{x_1, x_2} P[Z] \;+\; \mathcal{O}\left(\kappa^{N_t+3}\right) \;. \qquad (76)$$

The sum over the closed loops $\mathcal{C}$ is centre symmetric while the terms containing the Polyakov loop explicitly break the symmetry.

In following, we study the theory by means of Monte-Carlo methods. We used a heat-bath update for the link and matter fields. Since the matter action describing the gauge field matter interactions is local, we used a generalised Luescher-Weisz algorithm [54, 55] for the calculation of the Polyakov line expectation value.

We are now considering moderate values for κ, let us say $\kappa \leq 0.25$. We have already obtained (see figure 11) that for small β_{I} the Polyakov line is small. Increasing β_{I} above a critical value, the Polyakov line expectation value $\langle P \rangle$ rapidly takes large values. In fact, we find that, below the critical value, $\langle P \rangle$ is strictly vanishing in the infinite volume zero temperature limit (for fixed and finite aspect ratio) although $\langle P \rangle \neq 0$ for any finite system. This is illustrated in figure 14, left panel: the graph shows $\langle P \rangle$ for a N^3 lattice as a function of N. At least in the string-breaking phase for sufficiently small κ, we observe an exponential decrease of $\langle P \rangle$ with increasing N. In the Higgs phase (here for $\beta_{\mathrm{I}} = 0.6$ and $\kappa = 0.30$), we still observe a slight decrease of $\langle P \rangle$ with the system size. Whether the

33

Polyakov line expectation finally vanishes for large N cannot be inferred from the present data. Further investigations are left to future studies.

To monitor the deconfinement cross-over at finite temperatures, we have calculated $\langle P \rangle$ for a $6 \times N^2$ lattice as a function of β_I for the aspect ratios $4, 5, 6, 7$. Our numerical result is shown in figure 14, right panel. We observe a maximum of $\langle P \rangle$ for $\beta_\mathrm{I} = \beta_c \approx 0.75(5)$ and very little dependence on the system size N. We argue that $\beta_\mathrm{I} < \beta_c$, the explicit breaking of centre symmetry is weak, the physics of the regime might be similar to that of the symmetric theory for $\kappa = 0$, and that perturbation theory with respect to κ yields reliable results. On the hand for $\beta_\mathrm{I} \geq \beta_c$, centre symmetry breaking is strong and any similarities with the symmetric theory are lost although we always have $\chi = 1$ in (75). This is the parametric transition.

6 Centre-sector transitions in the $SU(2)$ Higgs theory

6.1 String breaking

In order to study centre sector transitions in a more realistic, i.e., more QCD-like, theory, we will study a theory where the "empty vacuum" features flat directions, where this vacuum symmetry collapses to the discrete centre symmetry upon the inclusion of quantum fluctuation and where the trivial centre-sector is favoured through the matter sector. In addition and for the first time in this paper, we will consider 4 Euclidean space-time dimensions.

The most simple such theory is a $SU(2)$ gauge theory with a scalar field (say Higgs) in the fundamental representation. This theory is accessible by means of lattice gauge theories with large statistical accuracy. The partition function is given by

$$Z = \int \mathcal{D}U \, \mathcal{D}\phi \, \mathcal{D}\phi^\dagger \, \exp\{S_\mathrm{Wil} + S_\mathrm{Higgs}\} \,, \tag{77}$$

$$S_\mathrm{Higgs} = \kappa \sum_{x,\mu} \mathrm{Re}\, \phi^\dagger(x)\, U_\mu(x)\, \phi(x+\mu) \; - \; \sum_x \left[\frac{1}{2}\, \phi^\dagger(x)\, \phi(x) \; + \; \lambda\, [\phi^\dagger(x)\, \phi(x)]^2 \right].$$

The parameter κ quantifies the interaction strengths of the scalar fields with the gauge sector, while λ gives rise to a quartic Higgs self-interaction.

The SU(2)-Higgs theory shares the so-called *string breaking* with QCD: at low temperatures and sufficiently weak gauge-matter interactions, the static quark anti-quark potential linearly rises at intermediate distances between the static quark antiquark pair while it flattens at asymptotic distances. A popular picture assumes that a colour electric flux tube still forms between a static quark antiquark pair and that this string breaks due to the creation of a Higgs anti-Higgs pair. Once the string is broken, there is little penalty in energy to increase any further the distance between the (screened) heavy quarks. The static
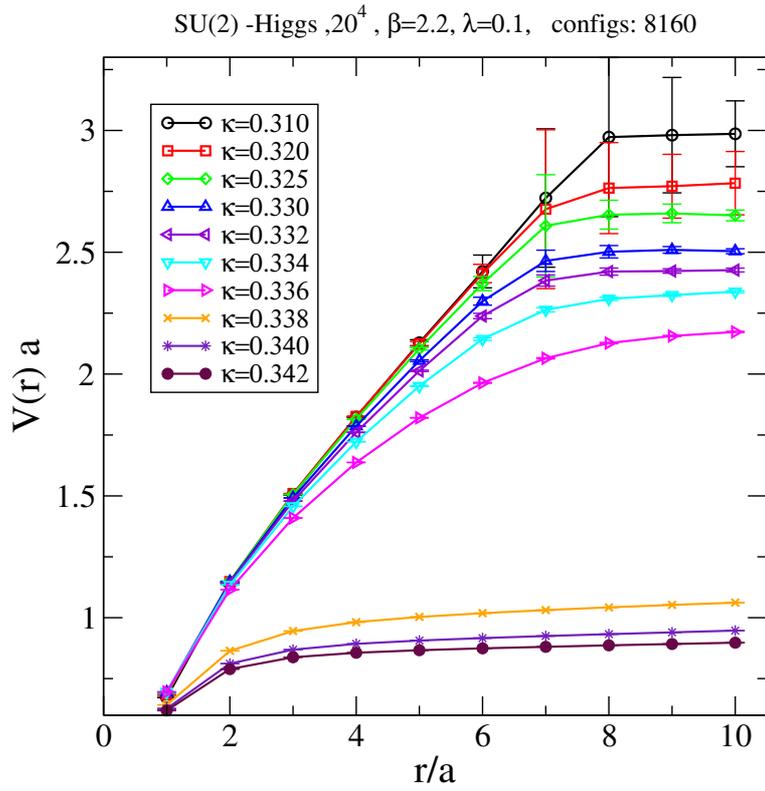
Figure 15: For the SU(2) Higgs theory ($\lambda = 0.1$) the static quark antiquark potential for a 20^4 lattice, $\beta_{\mathrm{Wil}} = 2.2$ and several values for κ, 8160 configurations per set.

potential approaches a constant. This also implies that the Polyakov line expectation is non-zero (even at low temperatures) and cannot serve any more as an order parameter.

The phase diagram has been qualitatively described in figure 11. On a more quantitative note, we have calculated the static potential by means of lattice gauge simulations. In order to ensure good ergodicity, we used the *local hybrid Monte-Carlo* update for the link fields as well as the scalar fields. In this paper, we work with $\lambda = 0.1$ and $\beta_{\text{Wil}} \in [2.2 \ldots 2.5]$ which roughly corresponds to the scaling window, at least, at small to moderate values κ.

To calculate the static quark potential, we here followed the two channel approach developed in [56, 57]. Using a 20^4 lattice, our results for the Wilson coupling $\beta_{\text{Wil}} = 2.2$, fixed quartic coupling $\lambda = 0.1$ and several values of κ is shown in figure 15. For each potential, 8160 independent lattice configurations contributed the relevant expectation values. For small values of κ, e.g. $\kappa < 0.336$, the string breaking scale can be intuitively set by an inspection of the graph: for $\kappa = 0.31$, we would set $r_b \approx 7\,a$. For larger values of κ, a gradual transition to the Higgs phase sets in, and a string breaking scale is hardly defined. It seems, however, that this scale cannot be pushed to small values by just altering the Higgs hopping parameter κ. If we fit the static potential for $r < r_b$ to $V(r) = a_0 + \sigma_{\text{int}} r + a_1/r$, we define the so-called intermediate string tension σ_{int}. For $\kappa = 0.31$, our estimate is

$$\sigma_{\text{int}} a^2 \approx 0.22(1)\,, \qquad r_b\,\sqrt{\sigma_{\text{int}}} \approx 3.3\,, \qquad r_b \approx 7.2\,\text{fm}\,, \tag{78}$$

if we assume the QCD value $\sigma_{\text{int}} \approx (440\,\text{MeV})^2$ to set the scale. We also point out that for κ values close to the transition line, e.g., for $\kappa = 0.336$, the string breaking scale is difficult to define. Here, the picture of a well defined short string might loose its validity.

6.2   Volume dependence of the Polyakov line expectation value

Integrating over the Higgs fields for a fixed link background yields an effective action for the links which is not anymore centre-symmetric. In order to get a first impression of the amount of *explicit breaking* we consider the normalised probability distribution for the spatial average of the Polyakov line,

$$W[p] \;=\; \big\langle\, \delta\big(p - \bar{P}[U]\big)\,\big\rangle\,, \tag{79}$$

where the expectation value is with respect to the partition function (12) and $\bar{P}[U]$ is the spatial average of the trace of the Polyakov line:

$$\bar{P}[U] \;=\; \frac{1}{V_3} \sum_{\boldsymbol{x}}\; \frac{1}{N_c}\, \text{tr}\, \mathcal{P}(\boldsymbol{x})\,. \tag{80}$$

Since in the low temperature phase the probability distribution of Polyakov line $\mathcal{P}$ is basically given by the Haar measure of the gauge group, the above distribution is divided by the reduced Haar measure distribution,

$$R(p) \;=\; W(p)/W_0(p)\,, \qquad W_0(p) \;=\; \frac{2}{\pi}\,\sqrt{1 - p^2} \tag{81}$$

36
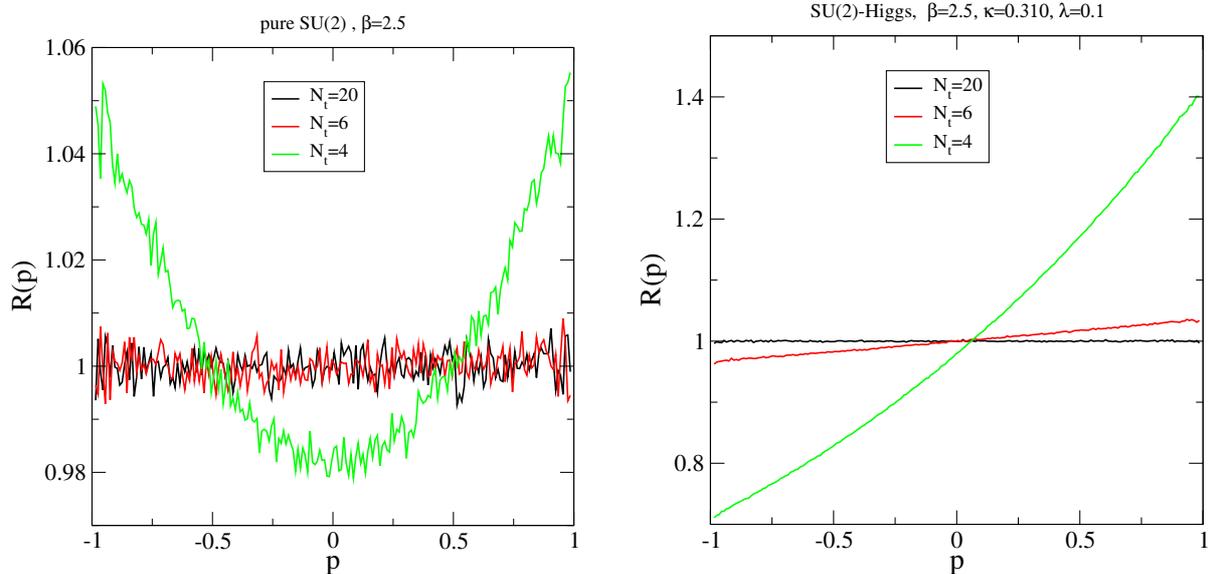
Figure 16: Ratio $R(p)$ of the Polyakov line distribution function over the Haar measure distribution for three different temperatures in pure Yang-Mills theory (left) and for the SU(2) Higgs theory on the $20^3 \times N_t$ lattice (right).

to extract any effects beyond the trivial distribution.

Let us first study pure Yang-Mills theory without Higgs matter. Our result is shown in figure 16, left panel. At zero temperatures, i.e., $N_s = N_t = 20$, for $\beta_{\text{Wil}} = 2.5$, this ratio is basically independent of p. We increase the temperature $T = 1/N_t a$ by decreasing the extent of the lattice in time direction. For $N_t = 6$ at $\beta_{\text{Wil}} = 2.5$, pure Yang-Mills theory is still in the confinement phase. Here we observe that deviations from the Haar measure distribution is still marginal. For $N_t = 4$, Yang-Mills theory is in the high temperature deconfinement phase, and significant deviations from the Haar measure distributions are clearly visible for large values for p. Here, a bias towards the centre elements, 1 and -1, is seen. In the infinite volume limit, tunneling between the centre sectors ceases to take place leading to a spontaneous breakdown of centre symmetry. It is, however, important to notice that the $N_t = 4$ distribution $W(p)$ is to a good extent symmetric under the reflection $p \to -p$ by virtue of the centre invariance of the functional integral. This signals good ergodicity of the algorithm even in the high temperature phase.

Let us now consider the SU(2) Higgs theory. We here used a $20^3 \times N_t$ lattice and $\beta_{\text{Wil}} = 2.5$, $\lambda = 0.1$ and $\kappa = 0.31$ which is somewhat below the critical value for the transition from the confining phase to the Higgs phase. Figure 16, right panel, summarises our findings. At very low temperatures, i.e., for $N_t = 20$, there is hardly any deviation from the Haar measure distribution visible. Still in the string-breaking phase at $N_t = 6$, there is a bias towards positive values of the Polyakov line noticeable. At high temperatures, such as for $N_t = 4$, above the deconfinement transition, this tendency is strongly amplified: the
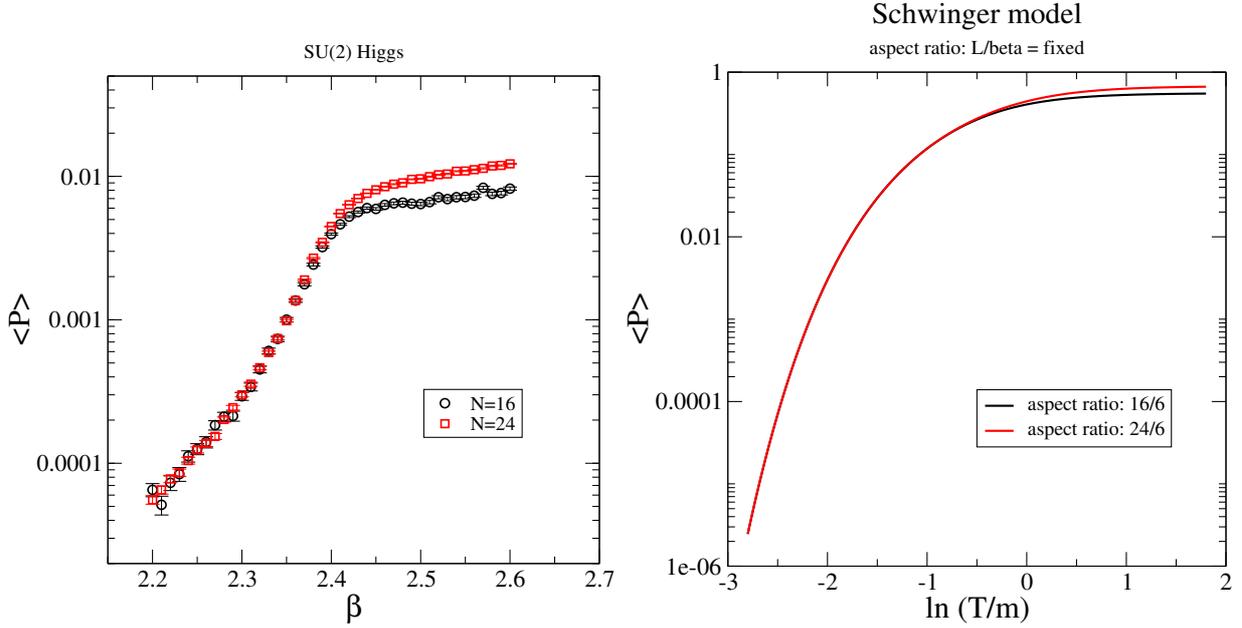
Figure 17: For a fixed aspect ratio N/N_t, the dependence of the Polyakov line expectation on Wilson β_{Wil} in the SU(2)-Higgs theory $\kappa = 0.31$, $\lambda = 0.1$, 2040 configurations per data point, (left panel). Same quantity as a function of $\ln T$ in the Schwinger model (right panel).

centre sector $z_1 = -1$ is even more suppressed while the probability for positive values of p reaches large values. In all cases (though less visible for $N_t = 20$), the centre symmetry $U \rightarrow U^c$, (8,9) is *explicitly* broken, and the Polyakov line probability distribution is no longer reflection symmetric, $W(p) \neq W(-p)$.

Apparently, the explicit centre symmetry breaking is much stronger at high temperatures than in vacuum. Does this mean that centre symmetry breaking is spontaneously broken at high temperatures? To answer this question, we have studied the the Polyakov line expectation value $\langle P \rangle$ for a fixed and finite aspect ratio, i.e., N/N_t, as a function of the system size. This can be easily achieved by using of fixed number of lattice points, $16^3 \times 6$ and $24^3 \times 6$, respectively, and to vary the Wilson β_{Wil}. The logarithm of the temperature T in relation to the fundamental renormalisation group scale such as the intermediate string tension σ is then roughly given by

$$\ln\left(\frac{T}{\sqrt{\sigma}}\right) = \ln\left(\frac{1}{N_t \sqrt{\sigma} a(\beta_{\mathrm{Wil}})}\right) \approx \gamma_1 \beta_{\mathrm{Wil}} + \text{constant},$$

where γ_1 is 1-loop Gell-Mann Low coefficient. For a pure SU(2) gauge theory, this coefficient would be $\gamma_1 = 3\pi^2/11$. Figure 17, left panel, shows $\langle P \rangle$ as a function of Wilson β_{Wil} using the Lüscher-Weisz method [54, 55] which is easily generalised to include the Higgs field. For small values of β_{Wil}, i.e., $\beta_{\mathrm{Wil}} < 2.4$, we roughly observe an exponential decrease of $\langle P \rangle$ with decreasing β_{Wil}. At high values, i.e., $\beta_{\mathrm{Wil}} \gtrsim 2.4$, $\langle P \rangle$ increases with increasing β_{Wil} at a

modest pace. Whether in this regime the dependence of $\langle P \rangle$ is still exponential (just with a much smaller slope) or whether the characteristic of this dependence has fundamentally changed cannot be concluded given the present set of data.

In pure SU(2) Yang-Mills theory and a $16^3 \times 4$, we would expect the deconfinement phase for $\beta_{\text{Wil}} \gtrsim 2.4$. It is tempting to conclude that the change of the dependence of $\langle P \rangle$ on β_{Wil} in this regime signals a spontaneous breaking of centre symmetry. We here argue that this conclusion is premature: figure 17, right panel, shows $\langle P \rangle$ as a function of $\ln T/m_\gamma$ (where m_γ is the induced photon mass which sets the scale) for the same fixed aspect ratio. Both curves are strikingly similar. While there is certainly no spontaneous breakdown of centre symmetry in the Schwinger model (this would lead to a Silver-Blaze problem as we pointed out in section 3), the large values of $\langle P \rangle$ merely indicates an overlap problem if we wish to address this model by means of Monte-Carlo methods.

6.3 Order parameter for centre-sector transitions

If we consider for the moment a given lattice configuration $\{U\}$ in pure Yang-Mills and its centre copy $\{^z U\}$, then these configurations are degenerate in action. If $\{U\}$ is an "empty vacuum" state, i.e., all contractible Wilson loops on the lattice yield the unit element, a path in configuration space can be found which deforms $\{U\}$ into $\{^z U\}$ without changing the action. For a generic lattice configurations, this no longer the case, and the crucial question is whether transitions between centre-sectors occurs at all in the infinite volume limit. The situation is aggravated if dynamical matter (transforming under the fundamental representation of the gauge group) is present which bias the trivial centre sector. We have partially answered this question by studying the volume dependence of the Polyakov line: in the string-breaking phase, the bias becomes negligible in the infinite volume limit, centre transitions do occur and the Polyakov line averages to zero; in the Higgs-phase explicit centre-symmetry breaking is strong and independent of the volume.

Our aim here will be to construct a sort of order parameter which is sensitive to the centre transitions. We do not expect that such an observable is built from local field operators and that it is an order parameter in the strict thermodynamics sense. It must necessarily be a non-local object which, however, nevertheless signals whether swapping the centre sectors can occur. To this aim, we divide the 3-volume into two parts of equal size, V_L and V_R and define the spatial average of the Polyakov line over each of the volumes:

$$\bar{P}_{L/R} = \frac{1}{V_{L/R}} \sum_{\boldsymbol{x} \in V_{L/R}} P(\boldsymbol{x}). \tag{82}$$

It is straightforward to assign a centre sector to each of the sublattices by the mapping

$$C(\bar{P}) = n, \qquad n : \left| \arg(\bar{P}) - \frac{2\pi n}{N_c} \right| \to \min , \tag{83}$$

where

$$\arg(\bar{P}) = \varphi \in]0, 2\pi] , \qquad \bar{P} = |\bar{P}| \exp\{\mathrm{i}\varphi\} .$$

39
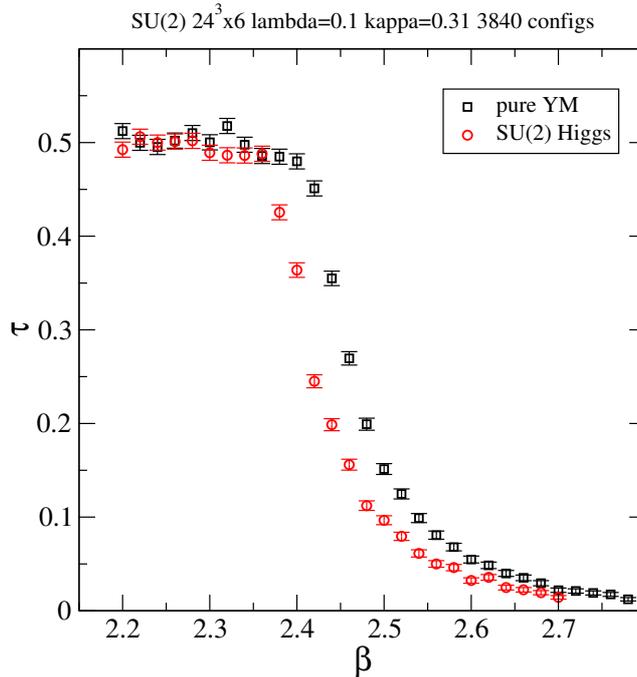
Figure 18: The tunneling coefficient for pure Yang-Mills theory and the SU(2) Higgs theory.

Let us then constrain the configurations in such a way that the left hand part of the universe belongs to centre-sector n while the right hand part has a reference to centre sector m. The ratio of partition functions between the constrained and the un-constrained theory defines the free energy F_{nm} for the mixing of the centre-sectors:

$$p_{nm} := \exp\{-F_{nm}/T\} \;\; = \;\; \frac{1}{N} \int \mathcal{D}U \, \mathcal{D}\phi \, \mathcal{D}\phi^\dagger \; \delta\Big(n, C(\bar{P}_L)\Big) \; \delta\Big(m, C(\bar{P}_R)\Big) \; \mathrm{e}^S \;, \quad (84)$$

$$N \;\; = \;\; \int \mathcal{D}U \, \mathcal{D}\phi \, \mathcal{D}\phi^\dagger \, \mathrm{e}^S \;.$$

The matrix p_{nm} can be interpreted as the probability to find sector n in the left half and sector m in the right half of the spatial universe. If the centre-symmetry is weakly broken in the string-breaking phase (or not broken at all in the infinite volume limit), the free energy F_{nm}, $n \neq m$ is finite (or might even tend to zero for an increasing system size), while the free energy diverges if the centre symmetry is strongly broken broken as e.g. in the Higgs phase or at high temperatures. This is basically due to the fact that the whole universe belongs to one centre sector, and configurations with $n \neq m$ have a very low probability.

Still measuring the free energy F_{nm} is hardly an easy task. Alternatively, we consider another intuitive measure for centre sector transitions: the probability τ that the volumes V_L and V_R belong to *different* sectors. We call τ the transition coefficient. It is directly

related to the free energy by

$$\tau \;=\; \sum_{n\neq m} p_{nm} \;=\; 1 \;-\; \sum_n p_{nn} \;=\; 1 \;-\; \sum_n \exp\{-F_{nn}/T\}\,. \tag{85}$$

In the infinite volume limit in the string-breaking phase, explicit centre symmetry breaking can be neglected implying

$$p_{nm} \;=\; \frac{1}{N_c^2} \qquad \Rightarrow \qquad \tau \;=\; 1 \;-\; \frac{1}{N_c}\,.$$

In the Higgs or the high temperature phase, the whole lattice belongs to one centre sector, and we find:

$$p_{nm} \;=\; \frac{1}{N_c}\,\delta_{nm} \qquad \Rightarrow \qquad \tau \;=\; 0\,.$$

We have numerically estimated the transition coefficient τ using a $24^3 \times 6$ lattice, $\kappa = 0.31$ and $\lambda = 0.1$. The parameter setting is such that the theory is in the string-breaking phase for a 24^4 lattice size. Figure 18 shows our findings for τ as a function β. We do find that for $\beta_{\mathrm{Wil}} \lesssim 2.35$ centre-sector transitions do occur with high probability while *one* centre-sector is observed throughout the lattice universe for high temperatures, i.e., $\beta_{\mathrm{Wil}} > 2.35$.

7 Conclusions

For SU(N) Yang-Mills in 4 dimensions on a torus, we started to investigate the "empty vacuum", i.e., the set of configurations for which all holonomies calculated for any contractible loop yields the unit element of the group. All these configurations produce zero field strength everywhere. We found a continuous set of *gauge in-equivalent* configurations related by a symmetry transformation. Including quantum fluctuations, the degeneracy of these states is lifted. The symmetry collapses to the well-known Z_N centre symmetry which divides the gluonic configurations into centre sectors. Transitions between the centre sectors turned out to be the key ingredient for *confinement*[3]. Including dynamical matter which transforms under the fundamental representation of the group, this centre symmetry is *explicitly broken.* Our central working hypothesis to start with was that transitions between centre sectors still take place in the so-called *hadronic* phase and that these transitions only cease to exist at high temperatures when the centre symmetry is also spontaneously broken (on top of the explicit breaking).

Before corroborating this picture in the sections 5 and 6, we studied the phenomenological impact in the Schwinger-model, since it allows for explicit analytical solutions, and in an SU(3) quark model for the sake of its relevance for QCD. For an even number of colours, it was firstly pointed out in [39, 40] that quarks acquire *periodic boundary conditions* in some of the centre sectors. For a finite chemical potential, the quarks then might

---

[3]although they do not explain the confinement energy scale of several hundred MeVs for QCD

undergo condensation due to Bose statistics. In analogy, this has been called *Fermi Einstein condensation* (FEC). We traced out the roots of FEC in the Schwinger model on the torus as finite chemical potential. We found that the phenomenological importance of the centre transitions is the solution of the *silver blaze problem*: centre transitions wipe any dependence of the partition function on the chemical potential as it must be since the physical states of the model carry no net baryon number.

We then studied an effective SU(3) quark model with constituent quark mass m which only interactions are with the gluonic background field specifying the centre sector. We verified that this very simple model already confines quarks: e.g., we considered the thermal energy density as a function of (low) temperatures and found that its lowest excitations are mesons of mass $\sim 2m$ rather than quarks with mass $\sim m$. By studying the centre sector weights (provided by the model), we found that the centre sectors democraticly contribute to the partition function in the hadronic phase while under extreme conditions basically only the trivial centre sector contributes implying that the model merges with the Fermi-gas model in the quark gluon plasma phase. Using the centre weight of the trivial centre sector as an order parameter, we were able to map out the phase diagram of the model as a function of the chemical potential and the temperature. We found that FEC is important at low temperatures and intermediate values of the chemical potential.

For FEC to happen in dense QCD, the central question is whether centre sector transitions do take place despite of the explicit breaking by matter fields. This question can be studied for vanishing chemical potential where Monte-Carlo simulations are readily available. Using a 3-dimensional $\mathbb{Z}_2$ gauge theory with Ising matter, we firstly studied the tension of a centre interface when the model is forced into the trivial centre sector (i.e., the sector for which the model is identical to the standard ferromagnetic Ising model). While the interface tension vanishes in the infinite-volume zero-temperature limit, it is finite at high temperatures when centre symmetry is spontaneously broken. Giving up the artificial constraint which ties the $\mathbb{Z}_2$ gauge theory with matter to the standard Ising model, we find that interface tension vanishes for any finite volume. Nevertheless, a detailed study of the Polyakov line expectation value reveals at rather small value (though non-zero) in the would-be confinement phase, and large values in the Higgs phase.

A theory which is more relevant for QCD, is the SU(2) gauge theory with dynamical matter. We have chosen a scalar Higgs field since it allows large statistic Monte-Carlo simulations (facilitated by e.g. the generalised Luescher-Weisz method) and at the same it explicitly breaks centre symmetry as quarks do. We firstly identified the region of the coupling space where the theory realises string breaking well within the size of our lattice. We then studied the extent of *explicit* centre symmetry breaking by calculating the Polyakov line distribution function. At high temperatures, the explicit breaking is largely amplified by an additional spontaneous breakdown. A study of the temperature dependence of the Polyakov line showed quite a similar behaviour as in the Schwinger model. This renders cumbersome any conclusion on the spontaneous centre symmetry breakdown since it is clearly absent in the Schwinger model. This calls for a new type of

order parameter which is designed to be a Litmus paper for centre transitions. For such an order parameter, we here proposed to map the Polyakov line to the centre sector for each half of the spatial lattice universe separately, and ask for the probability that a particular lattice configuration belongs to *different* centre sectors in each half. If this is the case, the theory certainly undergoes transitions between the centre sectors. Using this order parameter, we find clear numerical evidence in the SU(2) Higgs theory for a "hadronic" phase at small temperatures and a de-confined phase at high temperatures.

In conclusion, we found evidence that dynamical matter does not prevent centre sector transitions in QCD-like theories in the low temperature "hadronic" phase. These transitions only cease to exist at high temperatures when centre symmetry is also broken spontaneously. We highlighted the phenomenological impact of these centre transitions: in the Schwinger model, they solve the Silver-Blaze problem, and in an SU(3) quark model they lead to a new phase featuring Fermi Einstein condensation (FEC) for cold but dense matter. The FEC mechanism only uses fairly robust assumptions on the realisation of centre symmetry. Hence, FEC might also be at work in QCD at low temperatures and intermediate values of the chemical potential for which quarks are not yet liberated.

A   The Schwinger-model calculations

In this appendix we extend known results about the Schwinger model at finite temperature $T = 1/\beta$ [29] to the case with chemical potential $\mu \neq 0$. For related results on the Thirring model see [32]. We enclose the system in an interval with length L and impose periodic boundary conditions in the spatial direction.

A.1   Schwinger-proper time regularisation

Any gauge potential with vanishing instanton number on the two-dimensional torus can be decomposed as

$$A_0 = -\partial_1 \phi + \partial_0 \lambda + \frac{2\pi}{\beta} h_0 \quad , \quad A_1 = \partial_0 \phi + \partial_1 \lambda + \frac{2\pi}{L} h_1 \tag{86}$$

with constant toron fields h_0 and h_1. The determinant of the Dirac operator for massless fermions does not depend on λ and its ϕ-dependence follows from the axial anomaly [29]. Here we calculate the determinant for arbitrary toron fields h_μ and for a chemical potential

$\mu \neq 0$. For constant fields the Dirac operator possesses plane waves as eigenfunctions and its determinant can be written as an infinite product over all admitted momenta,

$$\det(\mathrm{i}\partial\!\!\!/_{h,\mu}) = \prod_{(m,n)\in\mathbb{Z}^2} D_{h,\mu}\,(m, E_n) \, , \tag{87}$$

The eigenfunctions are anti-periodic in time and periodic in space such that

$$D_{h,\mu}(m, E_n) = \left(\frac{2\pi}{\beta}\right)^2 \left(m + \tfrac{1}{2} - \gamma\right)^2 + E_n^2, \quad \gamma = h_0 + \frac{\mathrm{i}\beta}{2\pi}\mu, \tag{88}$$

where $LE_n = 2\pi|n - h_1|$. We introduce the fermionic effective action $\Gamma_{h,\mu}$ by

$$\Gamma_{h,\mu} = \ln\det(\mathrm{i}\partial\!\!\!/_{h,\mu}) \tag{89}$$

and obtain in Schwinger proper time regularisation

$$\Gamma_\Lambda(\mu, h) = \int_{1/\Lambda^2}^\infty \frac{ds}{s} \sum_{m,n} \mathrm{e}^{-sD_{h,\mu}(m,E_n)} \equiv \sum_n \Gamma_{\mathrm{fer}}(E_n, h, \mu) \, . \tag{90}$$

The terms in the last sum are given by the integral

$$\Gamma_{\mathrm{fer}}(E, h, \mu) = 2\int_E^\infty de\, e\, W(e) \, , \tag{91}$$

where the integrand contains the function

$$W(E) = \int_{1/\Lambda^2}^\infty ds \sum_m \exp\left\{-sD_{h,\mu}(m, E)\right\} \, .. \tag{92}$$

Now we can do the proper time integration. Since the resulting sum over m is convergent we may set $T/\Lambda = 0$ such that

$$W(E) = \mathrm{e}^{-E^2/\Lambda^2} \sum_m f(m, E) \quad \text{with} \quad f(m, E) = \frac{1}{D_{h,\mu}(m, E)} \, . \tag{93}$$

The sum over m can be rewritten with the help of the Poisson resummation formula

$$\sum_n f(m, E) = \sum_k \tilde{f}(k, E) \quad , \quad \tilde{f}(k, E) = \int dx\, \mathrm{e}^{2\pi \mathrm{i} kx}\, f(x, E) \, .$$

After a shift of the integration variable the last integral takes the form

$$\tilde{f}(k, E) = \frac{(-1)^k}{2\pi}\beta^2 \mathrm{e}^{2\pi \mathrm{i} kh_0} \int dx\, \frac{\mathrm{e}^{ikx}}{(x - \mathrm{i}\beta\mu)^2 + (\beta E)^2} \, . \tag{94}$$

The integral over x is known in closed form and the resulting sum over k can easily be computed and yields

$$\sum_k \tilde{f}(k, E) = \frac{1}{2E} \frac{d}{dE} \left\{ \beta E - \log \left(1 + e^{2\pi i \gamma - \beta E} \right) - \log \left(1 + e^{-2\pi i \gamma - \beta E} \right) \right\} . \tag{95}$$

Multiplied with $\exp(-E^2/\Lambda^2)$ this becomes the function $W(E)$ in (91). The μ-dependent part is UV-finite and hence we can safely remove the cutoff there leaving us with

$$\Gamma_\Lambda(\beta, \mu, h) = \beta E_\Lambda(L, h_1) + \Gamma_1(\beta, L, \mu, h) , \tag{96}$$

with a divergent zero-point energy E_Λ and a finite temperature correction

$$\Gamma_1(\beta, L, \mu, h) = \sum_n \ln \left\{ \left(1 + e^{2\pi i h_0} e^{-\beta(E_n + \mu)} \right) + \ln \left(1 + e^{-2\pi i h_0} e^{-\beta(E_n - \mu)} \right) \right\} . \tag{97}$$

In the zero-temperature limit we must recover the well-known Casimir energy of fermions on a circle with circumference L [58, 59],

$$\Gamma_\Lambda(\beta, L, \mu, h) \xrightarrow{\beta \to \infty} -\beta E_{\text{Cas}}, \quad E_{\text{Cas}} = -\frac{\pi}{6L} + \frac{2\pi}{L} \left(\frac{1}{2} - h_1 \right)^2 . \tag{98}$$

The Casimir energy is periodic in h_1 with period 1 and in the last formula we must assume $h_1 \in [0, 1]$. We conclude that the renormalised effective action is

$$\Gamma(\beta, L, \mu, h) = -\beta E_{\text{Cas}}(L, h_1) + \Gamma_1(\beta, L, \mu, h) . \tag{99}$$

Note that the energies E_n are proportional to $1/L$ such that Γ_1 depends only via the dimensionless parameter $\tau = \beta/L$ on the size L of the system.

A.2 θ-function representation and integration over toron fields

The effective action $\Gamma = \log \det(i\slashed{\partial})$ can be expressed in terms of the θ- and η-function [32]

$$\det(i\slashed{\partial}_{h,\mu}) = \frac{1}{\eta^2(i\tau)} \Theta \begin{bmatrix} h_1 - \frac{1}{2} \\ \gamma \end{bmatrix} (0, i\tau) \, \Theta \begin{bmatrix} h_1 - \frac{1}{2} \\ -\gamma \end{bmatrix} (0, i\tau) , \tag{100}$$

where γ is defined in (88) and we used the Dedekind eta-function

$$\eta(i\tau) = e^{-\pi\tau/12} \prod_{n>0} \left(1 - e^{-2\pi\tau n} \right), \quad \tau = \frac{\beta}{L} , \tag{101}$$

and the theta function [60]

$$\Theta \begin{bmatrix} \alpha \\ \gamma \end{bmatrix} (0, i\tau) = \sum_{n \in \mathbb{Z}} e^{-\pi\tau(n+\alpha)^2 + 2\pi i (n+\alpha)\gamma} \tag{102}$$

45

which has the product expansion

$$\frac{1}{\eta(\mathrm{i}\tau)}\Theta\begin{bmatrix}\alpha\\\gamma\end{bmatrix}(0,\mathrm{i}\tau) = \mathrm{e}^{2\pi\mathrm{i}\alpha\gamma}\mathrm{e}^{-\pi\tau\alpha^2+\pi\tau/12}$$
$$\cdot\prod_{n=1}^{\infty}\left(1+\mathrm{e}^{-2\pi\tau(n+\alpha-1/2)}\mathrm{e}^{2\pi\mathrm{i}\gamma}\right)\left(1+\mathrm{e}^{-2\pi\tau(n-\alpha-1/2)}\mathrm{e}^{-2\pi\mathrm{i}\gamma}\right).\quad(103)$$

Note that the determinant is invariant under large gauge transformations $h_\mu \to h_\mu + 1$.

Using the product expansion for the θ-function it follows at once that the effective action $\Gamma(\beta, L, \mu, h) = \log\det(\mathrm{i}\partial\!\!\!/_{h,\mu})$ has the series expansion (99). In the derivation we assumed that h_1 takes its values in the unit interval and this is why the h_1-periodicity of the determinant is not manifest. In the thermodynamic limit we find the following expression for the free energy density f in $Z = \exp(-\beta L f)$:

$$f \xrightarrow{L\to\infty} -\frac{1}{\pi\beta}\int_0^\infty dp\,\log\left[\left(1+\mathrm{e}^{2\pi\mathrm{i}h_0}\mathrm{e}^{-\beta(p+\mu)}\right)\left(1+\mathrm{e}^{-2\pi\mathrm{i}h_0}\mathrm{e}^{-\beta(p-\mu)}\right)\right]$$
$$= \frac{1}{\pi\beta^2}\left[\mathrm{dilog}\left(1+\mathrm{e}^{2\pi\mathrm{i}h_0-\beta\mu}\right)+\mathrm{dilog}\left(1+\mathrm{e}^{-2\pi\mathrm{i}h_0+\beta\mu}\right)\right].\quad(104)$$

For $L/\beta \to \infty$ the free energy density does not depend on the constant gauge field h_1, as expected. When one varies the constant gauge field h_0 (or equivalently the boundary condition in the temporal direction) then one smoothly interpolates between free fermions and free bosons or between a Fermi-Dirac and a Bose-Einstein distribution.

In a gauge theory we must average over all gauge fields and in particular we must integrate the fermionic determinant over the constant gauge fields as well. The integral of (100) over h_1 can be done explicitly. If m, n are the summation indices in the double sum (100) we change summation indices according to $m = p + q$ and $n = q$. The sum over q together with the h_1-integral over $[0, 1]$ turns into an integral over $[-\infty, \infty]$ and yields the simple result (27). The final integration over h_0 is easily performed and yields the μ-independent result (28) for the averaged determinant $\int dh_0 dh_1 \det(\mathrm{i}\partial\!\!\!/_{h,\mu})$.

A.3   Polyakov loops

Let us finally calculate the expectation values of product of Polyakov loops

$$P_q(u) = \mathrm{e}^{iq\int dx^0 eA_0(x^0,u)} = \mathrm{e}^{2\pi iq h_0}\mathrm{e}^{-ieq\int \partial_u\phi(x^0,u)dx^0}\quad(105)$$

corresponding to static charges $q \in \mathbb{Z}$. In particular $P_{-q} = \bar{P}_q$. First we do the integration over the harmonics. With the help of (27) we obtain

$$\int dh_0 dh_1 \det\left(\mathrm{i}\partial\!\!\!/_{h,\mu}\right)\prod P_{q_i}(u_i) = \frac{1}{\sqrt{2\tau}}\frac{1}{\eta^2(\mathrm{i}\tau)}\mathrm{e}^{-\pi\tau Q^2/2+\beta\mu Q}\mathrm{e}^{-i\int d^2x\,j(x)\phi(x)}$$

with total charge $Q = \sum q_i$ and source

$$j(x) = e \sum_i q_i \delta'(x^1 - u_i). \tag{106}$$

The functional integral over ϕ has been done previously in [29] and yields

$$\left\langle \prod_i P_{q_i}(u_i) \right\rangle = \prod_i \langle P_{q_i} \rangle \, \mathrm{e}^{-\beta \sum_{i \neq j} q_i q_j V(|u_i - u_j|)} \tag{107}$$

with expectation values (33) for the individual Polyakov loops and periodic potential

$$V(|u|) = \frac{\pi m_\gamma}{4} \frac{\cosh\left(\frac{m_\gamma}{2}(L - 2|u|)\right)}{\sinh\left(\frac{m_\gamma L}{2}\right)}, \quad |u| \leq L. \tag{108}$$

The potential energy decreases exponentially fast for large separations of the charges

$$V(|u|) \sim \frac{\pi m_\gamma}{4} \, \mathrm{e}^{-m_\gamma L/2}. \tag{109}$$

B   Local-hybrid Monte Carlo for the Higgs sector

For the update the scalar field in accordance to the functional integral (77), we here discuss the Local Hybrid-MC (LHMC) scheme. Assume that $\phi(x)$ is chosen for the update. The LHMC Hamiltonian is given by

$$H = \frac{1}{2} \pi^\dagger \pi + S_L(\phi, \phi^\dagger). \tag{110}$$

To set up the LHMC scheme, it is convenient to work with real variables, i.e., $\pi = R + iS$, $\phi = r + is$, $s, S, r, R \in \mathbb{R}$. The Hamilton-Jacobi equations of motion are given by

$$\dot{r} = \frac{\partial H}{\partial R} = R, \qquad \dot{s} = \frac{\partial H}{\partial S} = S, \tag{111}$$

$$\dot{R} = -\frac{\partial S_L}{\partial r} = -\frac{\partial S_L}{\partial \phi} - \frac{\partial S_L}{\partial \phi^\dagger}, \qquad \dot{S} = -\frac{\partial S_L}{\partial s} = -i\left[\frac{\partial S_L}{\partial \phi} - \frac{\partial S_L}{\partial \phi^\dagger}\right]. \tag{112}$$

It is easy to check that the above equations imply $\dot{H} = 0$. Combining both equations in (112) yields:

$$\dot{\pi} = \dot{R} + i\dot{S} = -2\frac{\partial S_L}{\partial \phi^\dagger}, \qquad \dot{\phi} = \dot{r} + i\dot{s} = \pi. \tag{113}$$

For the action in (77), the terms of S_{Higgs} which depend on $\phi(x)$ or $\phi^\dagger(x)$ give rise to

$$\begin{aligned}
S_L &= -\frac{\kappa}{2} \sum_\mu \left[\phi^\dagger(x)\, U_\mu(x)\, \phi(x+\mu) + \phi^\dagger(x)\, U_\mu^\dagger(x-\mu)\, \phi(x-\mu)\right] \\
&\quad - \frac{\kappa}{2} \sum_\mu \left[\phi^\dagger(x-\mu)\, U_\mu(x-\mu)\, \phi(x) + \phi^\dagger(x+\mu)\, U_\mu^\dagger(x)\, \phi(x)\right] \\
&\quad + \frac{1}{2} \phi^\dagger(x)\, \phi(x) + \lambda\, [\phi^\dagger(x)\, \phi(x)]^2.
\end{aligned}$$

47

Hence, defining

$$B(x) \ = \ \sum_\mu \Big[U_\mu(x)\,\phi(x+\mu) \ + \ U_\mu^\dagger(x-\mu)\,\phi(x-\mu) \Big] \, , \tag{114}$$

we finally find:

$$\dot\phi \ = \ \pi \, , \qquad \dot\pi \ = \ \kappa\,B(x) \ - \ \phi(x)\Big[1 + 4\,\lambda\,\phi^\dagger(x)\phi(x) \Big] \, . \tag{115}$$

References

[1] F. Karsch, Lect. Notes Phys. **583** (2002) 209-249. [hep-lat/0106019].

[2] G. Boyd, J. Engels, F. Karsch, E. Laermann, C. Legeland, M. Lutgemeier, B. Petersson, Nucl. Phys. **B469** (1996) 419-444. [hep-lat/9602007].

[3] M. Cheng, N. H. Christ, S. Datta, J. van der Heide, C. Jung, F. Karsch, O. Kaczmarek, E. Laermann *et al.*, Phys. Rev. **D77** (2008) 014511. [arXiv:0710.0354 [hep-lat]].

[4] E. Shuryak, Prog. Part. Nucl. Phys. **62** (2009) 48-101. [arXiv:0807.3033 [hep-ph]].

[5] A. D. Frawley, T. Ullrich, R. Vogt, Phys. Rept. **462** (2008) 125-175. [arXiv:0806.1013 [nucl-ex]].

[6] B. Svetitsky, L. G. Yaffe, Nucl. Phys. **B210** (1982) 423.

[7] B. Svetitsky, Phys. Rept. **132** (1986) 1-53.

[8] J. Greensite, Prog. Part. Nucl. Phys. **51** (2003) 1. [hep-lat/0301023].

[9] L. Del Debbio, M. Faber, J. Giedt, J. Greensite, S. Olejnik, Phys. Rev. **D58** (1998) 094501. [hep-lat/9801027].

[10] K. Langfeld, H. Reinhardt, O. Tennert, Phys. Lett. **B419** (1998) 317-321. [arXiv:hep-lat/9710068 [hep-lat]].

[11] V. I. Zakharov, *Matter of resolution: From quasiclassics to fine tuning*, [hep-ph/0602141].

[12] K. Langfeld, E. -M. Ilgenfritz, Nucl. Phys. **B848** (2011) 33-61. [arXiv:1012.1214 [hep-lat]].

[13] K. Langfeld, O. Tennert, M. Engelhardt, H. Reinhardt, Phys. Lett. **B452** (1999) 301. [hep-lat/9805002].

[14] M. Engelhardt, K. Langfeld, H. Reinhardt, O. Tennert, Phys. Rev. **D61** (2000) 054504. [hep-lat/9904004].

[15] K. Langfeld, Phys. Rev. **D67** (2003) 111501. [hep-lat/0304012].

[16] J. B. Kogut, D. K. Sinclair, S. J. Hands, S. E. Morrison, Phys. Rev. **D64** (2001) 094505. [hep-lat/0105026].

[17] B. Wellegehausen, A. Maas, L. von Smekal, A. Wipf, in preparation.

[18] P. de Forcrand, PoS **LAT2009** (2009) 010. [arXiv:1005.0539 [hep-lat]].

[19] O. Schnetz, M. Thies, K. Urlichs, Annals Phys. **314** (2004) 425-447. [hep-th/0402014].

[20] O. Schnetz, M. Thies, K. Urlichs, Annals Phys. **321** (2006) 2604-2637. [hep-th/0511206].

[21] C. Boehmer, M. Thies, K. Urlichs, Phys. Rev. **D75** (2007) 105017. [hep-th/0702201].

[22] J. S. Schwinger, Phys. Rev. **128** (1962) 2425-2429.

[23] L.S. Brown, Nuovo Cimento **29** (1963) 617-643

[24] J. Lowenstein, A. Swieca. Ann. Phys. **68** (1971) 172-195;

[25] A. Casher, J. B. Kogut, L. Susskind, Phys. Rev. **D10** (1974) 732-745.

[26] N. Manton, Ann. Phys. **159** (1985) 220-251

[27] S. Iso, H. Murayama, Prog. Theor. Phys. **84** (1990) 142-163.

[28] H. Joos, Helv. Phys. Acta **63** (1990) 670-682.

[29] I. Sachs and A. Wipf, Helv. Phys. Acta **65** (1992) 652-678. [arXiv:hep-th/1005.1822]

[30] A. V. Smilga, Phys. Lett. **B278** (1992) 371-376.

[31] S. Azakov, Fortsch. Phys. **45** (1997) 589-626. [hep-th/9608103].

[32] I. Sachs and A. Wipf, Annals Phys. **249** (1996) 380-429. [arXiv:hep-th/9508142]

[33] R. F. Alvarez-Estrada, A. Gomez Nicola, Phys. Rev. **D57** (1998) 3618-3633. [hep-th/9710227].

[34] A. Fayyazuddin, T.H. Hansson, M.A. Nowak, J.J.M. Verbaarschot, I. Zahed, Nucl. Phys. **B425** (1994) 553-578. [hep-ph/9312362]

[35] L. McLerran, R. D. Pisarski, Nucl. Phys. **A796** (2007) 83-100. [arXiv:0706.2191 [hep-ph]].

[36] L. McLerran, K. Redlich, C. Sasaki, Nucl. Phys. **A824** (2009) 86-100. [arXiv:0812.3585 [hep-ph]].

[37] K. Fukushima, D. E. Kharzeev and H. J. Warringa, Phys. Rev. D **78** (2008) 074033 [arXiv:0808.3382 [hep-ph]].

[38] P. V. Buividovich, M. N. Chernodub, E. V. Luschevskaya and M. I. Polikarpov, Phys. Rev. D **80** (2009) 054503 [arXiv:0907.0494 [hep-lat]].

[39] K. Langfeld, B. H. Wellegehausen and A. Wipf, Phys. Rev. D **81** (2010) 114502 [arXiv:0906.5554 [hep-lat]].

[40] K. Langfeld, *Centre-sector tunneling, confinement and the quark Fermi surface*, invited talk at the workshop on "Chiral symmetry and confinement in cold dense quark matter", ECT, Trento, July 19 - 23, 2010.

[41] E. Bilgici, F. Bruckmann, J. Danzer, C. Gattringer, C. Hagen, E. M. Ilgenfritz, A. Maas, Few Body Syst. **47** (2010) 125-135. [arXiv:0906.3957 [hep-lat]].

[42] A. Keurentjes, A. Rosly and A. V. Smilga, Phys. Rev. D **58** (1998) 081701 [arXiv:hep-th/9805183].

[43] K. G. Selivanov, Phys. Lett. B **471** (1999) 171 [arXiv:hep-th/9909136].

[44] M. Schaden, Phys. Rev. D **71** (2005) 105012 [arXiv:hep-th/0410254].

[45] S. Blau, M. Visser and A. Wipf, Int. J. Mod. Phys. **A4** (1989) 1467-1484

[46] T. D. Cohen, Phys. Rev. Lett. **91** (2003) 222001 [arXiv:hep-ph/0307089].

[47] L. Alvarez-Gaume, G.M. Moorhead C. Vafa, Commun. Math. Phys. **106** (1986) 1-40

[48] F. J. Wegner, J. Math. Phys. **12** (1971) 2259-2272.

[49] E. H. Fradkin, S. H. Shenker, Phys. Rev. **D19** (1979) 3682-3697.

[50] M. Creutz, Phys. Rev. **D21** (1980) 1006.

[51] G. A. Jongeward, J. D. Stack, Phys. Rev. **D21** (1980) 3360.

[52] E. Brezin, J. M. Drouffe, Nucl. Phys. **B200** (1982) 93.

[53] P. de Forcrand, B. Lucini, M. Vettorazzo, Nucl. Phys. Proc. Suppl. **140** (2005) 647-649. [hep-lat/0409148].

[54] M. Luscher and P. Weisz, JHEP **0109** (2001) 010 [arXiv:hep-lat/0108014].

[55] M. Luscher and P. Weisz, JHEP **0207** (2002) 049 [arXiv:hep-lat/0207003].

[56] O. Philipsen and H. Wittig, Phys. Rev. Lett. **81** (1998) 4056 [Erratum-ibid. **83** (1999) 2684] [arXiv:hep-lat/9807020].

[57] F. Knechtli and R. Sommer [ALPHA collaboration], Phys. Lett. B **440** (1998) 345 [arXiv:hep-lat/9807022].

[58] M. Bordag, U. Mohideen and V.M. Mostepanenko, Phys.Rept. **353** (2001) 1 [arXiv:quant-ph/0106045]

[59] C. Kiefer and A. Wipf, Ann. Phys. **236** (1994) 241-285. [arXiv:hep-th/9306161]

[60] D. Mumford, Tata lectures on Theta Functions, Birkhäuser, Springer 1994